Moho depth and crustal composition in Southern Africa
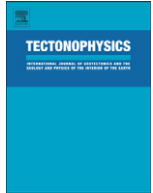
Soliman, Mohammad Youssof Ahmad; Thybo, Hans; Artemieva, Irina; Levander, Alan

Review Article

Moho depth and crustal composition in Southern Africa

M. Youssof [a,*], H. Thybo [a], I.M. Artemieva [a], A. Levander [b]

[a] Geology Section, IGN, University of Copenhagen, DK-1350 Copenhagen-K, Denmark
[b] Department of Earth Science, Rice University, Houston, TX 77005-1892, USA

ARTICLE INFO

ABSTRACT

We present new results on structure, thickness, and composition of the crust in southern Africa based on 6300 seismic receiver functions at 85 stations. Application of Hk-stacking to the entire SASE dataset and use of multi-frequency bands improve resolution substantially. We observe a highly heterogeneous crustal structure with short wavelength variations in thickness (H), Vp/Vs-ratio (composition), and Moho sharpness, which defines ~20 blocks that do not everywhere coincide with surface tectonic features. In the Zimbabwe Craton, the Tokwe block has H = 35–38 km and Vp/Vs = 1.74–1.79 whereas the thicker crust in the Tati block (H = 47–51 km) may be related to deformation of the Archean crust along the cratonic margin. Two distinct crustal blocks with similar crustal thickness (42–46 km) but significantly different Vp/Vs-ratios are recognized in the Limpopo Belt. Extreme values of 1.90–1.94 at the dyke swarms in eastern Limpopo, and 1.84 at the Olifants River Dyke Swarm and easternmost Bushveld Intrusion Complex (BIC) indicate voluminous magmatic intrusions in the whole crust. We find no evidence for magmatic intrusions in the central (inferred) part of BIC, where the crust is thick (45–50 km) and Vp/Vs is low (1.68–1.70). This thick crustal root may have deflected rising magmas to form the two BIC lobes. Most of central Kaapvaal has thin (35–40 km) crust and Vp/Vs ~ 1.74. These characteristics are similar to the Tokwe block in Zimbabwe Craton and may indicate delamination of pre-existing lower crust, which is further supported by a very sharp Moho transition. The exposed cross-section in the Vredefort impact crater is non-representative of cratonic crust due to shallow Moho (34 km) and high Vp/Vs ~ 1.80 attributed to shock metamorphism. High Vp/Vs = 1.76 is typical of the Witwatersrand Basin, and anomalously low Vp/Vs = 1.66–1.67 marks the Kaapvaal–Kheis–Namaqua transition. Highly heterogeneous crust, both in thickness and Vp/Vs-ratio is typical of the Namaqua–Natal and Cape Fold Belts.

© 2013 Elsevier B.V. All rights reserved.

Contents

* Corresponding author.
  E-mail addresses: ms@geo.ku.dk, mohammadyoussof@gmail.com (M. Youssof).

1. Introduction

It is generally accepted that continental crust is formed chiefly along plate margins in relation to subduction of oceanic crust and accretion of island or continental arcs, although details are still debated (Amelin et al., 1999; Arculus, 1999; Fyfe, 1978; Hawkesworth and Kemp, 2006; Hawkesworth et al., 2013; Rudnick and Fountain, 1995; Rudnick and Gao, 2003; Thybo and Artemieva, 2013). Greenstone belts with intervening gray gneisses, widespread in southern Africa and other cratons worldwide, are classic examples of Archean continental crust that has been generated in volcanic arcs and later assembled into the cratons by processes similar to modern plate tectonics (Condie, 1997; de Wit et al., 1992).

It has for long been recognized that the cratons of southern Africa (the Kaapvaal and Zimbabwe Cratons and the intervening late Archean Limpopo Mobile Belt, termed altogether the Kalahari Craton (Clifford, 1970)) comprise some of the oldest continental crust with ages as old as ca. 3.5–3.7 Ga (Cahen et al., 1984; Hamilton et al., 1979; Thomas et al., 1993) (Fig. 1). It is thus of little surprise that crustal structure of the Kalahari Craton has been the focus of numerous geophysical, geochemical, and geodynamic studies that aimed at understanding the processes of formation and evolution of continental crust in different tectonic environments (Cooper, 1990; Kröner, 1976). Two, apparent "end-member", concepts for the structure of cratonic continental crust have been proposed about two decades ago based on the limited seismic data available at that time. One concept proposes that Proterozoic crust is thicker than Archean crust, largely due to the presence of a thick lower crustal layer in Proterozoic crust which is absent in Archean crust (Durrheim and Mooney, 1991, argued by Wever, 1992). The other concept suggests that, on average, the thickness of Archean and Proterozoic crust is approximately the same (Rudnick and Fountain, 1995). It is clear, however, that the present-day crustal structure of Precambrian cratons reflects a long evolutionary history with modification by numerous tectonic and magmatic processes, and thus no simple age relationships should be expected, but rather strong structural and compositional heterogeneity at all scales, such as reported, for example, for the Indian Craton (Gupta et al., 2003).

To image the crust and upper mantle beneath the Archean and Proterozoic parts of the Kalahari Craton and the adjacent Phanerozoic provinces, the Southern African Seismic Experiment (SASE, Fig. 2) was designed with an array of broad-band stations deployed at 82 sites in 1997–1999 (Carlson et al., 1996). However, the absence of regional seismicity and the large lateral spacing between stations in the SASE array limit the resolution of the crustal models constrained by teleseismic

body wave and surface wave tomography. In particular, the P-wave velocity structure of the upper 50 km (the crust) cannot be resolved by teleseismic body wave tomography (James et al., 2001a, 2001b). Similarly, surface wave tomography can only produce velocity models at periods longer than ~20 s, which mainly constrains the upper mantle
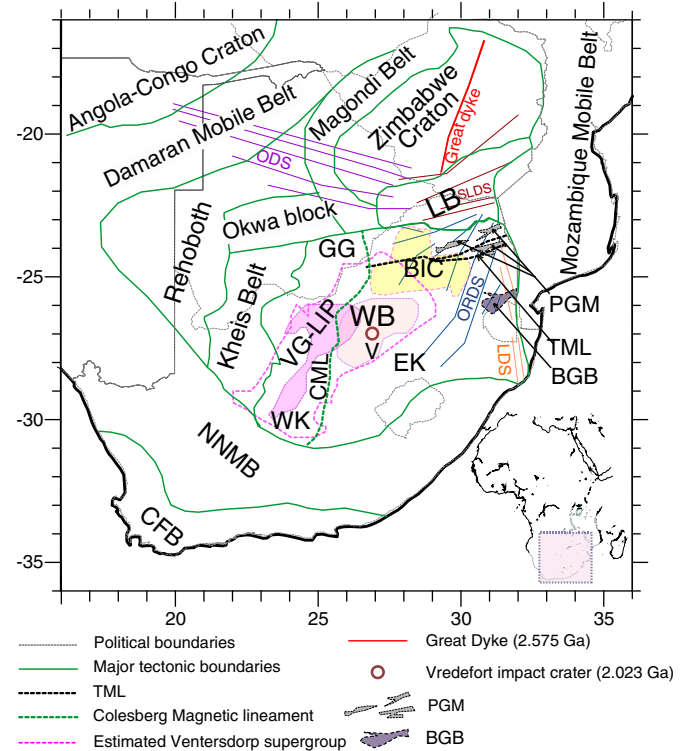
Fig. 1. Tectonic map of the southern Africa terranes. Abbreviations for the tectonic terranes are: BGB = Barberton Greenstone Belt (3.45–3.25 Ga); BIC = Bushveld Intrusion Complex (2.05 Ga); CFB = Cape Fold Belt; CML = Colesberg Magnetic Lineament; dyke swarms: ODS = Okavango(~180 Ma & Pt), SLDS = Save-Limpopo(~1.4 Ga), LDS = Lebombo (~1.4 Ga), ORDS = Olifants River (0.8–1.7 Ga & ~2.5–2.9 Ga); EK = Eastern Kaapvaal Craton (3.4–3.7 Ga); GG = Gaborone granites (ca. 2.0 Ga); LB = Limpopo Belt (Ga 2.7); NNMB = Namaqua–Natal Mobile Belt; PGM = Pietersburg–Giyani–Murchison Belt includes MGB = Murchison Greenstone Belt (3.2–3.0 Ga) and PGT = Pietersburg–Giyani terrane (>3Ga); TML = Thabazimbi–Murchison Lineament Belt (2.7 Ga); WB = Witwatersrand Basin (2.05 Ga); V = Vredefort impact structures(2.023 Ga); VG–LIP = Ventersdorp group (graben 2.7 Ga; 2.05 Ga) and LIP (2.05 Ga); WK = Western Kaapvaal Craton(3.1–3.3 Ga).
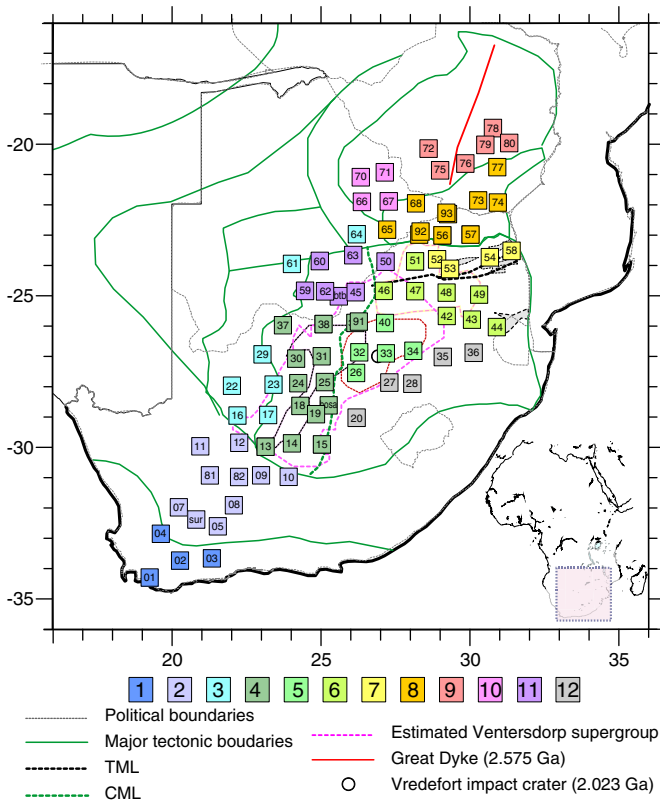
Fig. 2. Map showing the locations of the 82 stations of the SASE array and 3 permanent GSN seismic stations. Note that three pairs of stations are located at almost the same coordinates: stations SA91,SA92, and SA93 are behind stations SA39, SA55, and SA69. Color code for the SASE array corresponds to the numbering of tectonic blocks as follows. 1: Cape Fold Belt (CFB), 2: Namaqua–Natal Mobile Belt (NNMB), 3: Kheis–Okwa Mobile Belt (KOMB), 4: Western Kaapvaal — Ventersdorp LIP (VG-LIP), 5: Central Kaapvaal — Witwatersrand Basin (WRB), 6: Northern Kaapvaal — Bushveld Igneous Complex (BIC), 7: Northern Kaapvaal — Pietersburg–Giyami–Murchison (PGM), 8: Limpopo Mobile Belt (LB), 9: Zimbabwe Craton–Tokwe gneiss block (ZCT), 10: W Zimbabwe Craton–Tati Granite–Greenstone (TGGT), 11: NW Kaapvaal–Late Archean Gaberone granites (GG), 12: Eastern Kaapvaal (EK).

The high quality seismic data from the SASE experiment has provided a basis for several detailed studies of crustal architecture of the Kalahari Craton. Due to technical limitations of the different approaches, these results suggest that the crust beneath the Kaapvaal and Zimbabwe Cratons is relatively thin (35–40 km) with a flat Moho-discontinuity (Nair et al., 2006; Nguuri et al., 2001; Niu and James, 2002; Yang et al., 2008). In agreement with earlier conclusions (Durrheim and Mooney, 1991), a large velocity and density contrast at the Moho may be attributed to the lack of a high velocity mafic layer in the lower crust. In contrast, the crust of tectonically reworked blocks (in particular the northern Kaapvaal Craton and the Limpopo Mobile Belt) is significantly thicker (>45 km) and more mafic than the crust of central Kaapvaal. However, deep crustal roots with the presence of thick mafic underplated material, as documented in other cratons, have not been reported so far in southern Africa. For example, recent seismic studies in the Archean terranes of North America and the Baltic Shield indicate the presence of an up-to 60 km thick crust with a very thick (10–25 km) high velocity mafic layer (Vp ~ 7.2–7.5 km/s beneath Central Finland and 7.5–7.9 km/s beneath the Medicine Hat-Wyoming blocks) (Clowes et al., 2002; Peltonen et al., 2006). In both cases, seismic models are supported by petrologic data from lower crustal xenoliths and the high velocity basal layer is interpreted as mafic underplating (Thybo and Artemieva, 2013).

Here we present a new model of the crustal thickness of the Kalahari Craton based on the first full Hk-stacking interpretation of data recorded by all 82 broadband seismic stations of the SASE experiment and three permanent stations in southern Africa. Our approach is based on Receiver Function (RF) analysis of P to S conversions derived from the best quality data by application of the Hk-stacking technique to the main converted phases and their multiples. As a result, we distinguish significant small-scale heterogeneities in the thickness and chemical composition of the crust as reflected in our new Vp/Vs crustal model for the entire array. We further compare our new comprehensive crustal model with other regional models of crustal thickness and Vp/Vs based on the SASE array and discuss reasons for model differences, as well as geodynamic interpretations of their robust and well-constrained features in relation to regional tectonic evolution.

2. Tectonic setting

Southern Africa comprises a mosaic of the best-preserved and exposed crustal blocks which were assembled in early–late Archean and subsequently modified by several major Precambrian and Phanerozoic tectonothermal events (Cooper, 1990; de Wit et al., 1992; Thomas et al., 1993). It is outside of the scope of this paper to present an overview of the tectonic evolution of the region and we limit our brief summary to the major events which may have affected the crustal structure (Fig. 1).

2.1. Early Archean formation of cratonic nuclei

- The cratonic nuclei started with regional formation of continental lithosphere (the granite–greenstone terranes of the Kaapvaal and Zimbabwe Cratons, 3.2–3.7 Ga) through intra-oceanic obduction of hydrated Archean oceanic crust. The oldest crust is ca. 3.4–3.7 Ga in the ancient core of the eastern–southeastern parts of the Kaapvaal Craton (the Swaziland Ancient Gneiss Complex and the Komati greenstones of the Barberton Greenstone Belt) (Cahen et al., 1984; Hamilton et al., 1979; Thomas et al., 1993) and ca. 3.5 Ga in the gneisses of the oldest known Tokwe block of the southeastern Zimbabwe Craton (Rollinson, 1993; Smith et al., 2009);
- The initial crustal formation was amalgamation of oceanic terranes, granitoid formation, and cratonization (3.1–3.3 Ga) (de Wit et al., 1992); which lead to the formation of a single, coherent crustal block in the southern and central parts of the Kaapvaal Craton by ca. 3.1 Ga (Thomas et al., 1993).

instead of the crust (Dahlen and Tromp, 1998; Ritzwoller and Levshin, 1998). To improve the resolution, the small, dense Kimberley Telemetered Array (KTA) was additionally deployed for five months during the second year of the SASE deployment near a large population of kimberlite pipes. However, the KTA array covers only a very small portion of the Kaapvaal Craton and cannot constrain crustal structure on craton scale.

Given the geometry of the SASE array, the crustal structure, including the Moho depth, of southern Africa can best be inferred from teleseismic RF analysis (e.g., Gore et al., 2009; Nair et al., 2006; Nguuri et al., 2001; Niu and James, 2002; Vinnik et al., 2012), combined with surface wave tomography (Kgaswane et al., 2009, 2012), or from interpretation of regional body waves (e.g., Kwadiba et al., 2003; Wright et al., 2004), finite-frequency surface wave tomography (Chevrot and Zhao, 2007), ambient and teleseismic tomography (Yang et al., 2008), as well as from a combination of seismic and potential field data (Webb et al., 2004). RF analysis provides high vertical resolution of the crustal structure, in particular by including analysis of the free-surface reverberation phases (Niu and James, 2002; Shibutani et al., 1996). Compared to the RF models, the tomography models have weaker lateral and vertical resolution and provide a smoother image of the crustal structure, although ambient noise tomography yields a reasonable vertical resolution for the crust at periods from 6 s to 40 s (Yang et al., 2008).

2.2. Late Archean Craton formation, stabilization, and rifting

- Regional extension and formation of rift basins (e.g., the Dominion, the Witwatersrand, and the Ventersdorp basins) in the central and southern parts of the ancient nucleus (2.7–3.1 Ga) (de Wit et al., 1992);
- Development of a rifted continental margin along the northern and western margins of the Kaapvaal ancient core, subsequent continental or arc-collision (2.7–2.9 Ga) along the Colesburg Lineament which separates the late Archean Western and the Mid-Archean Central segments of the Kaapvaal Craton (de Wit et al., 1992);
- Amalgamation of the northern (2.9–3.0 Ga) and southern blocks of the Kaapvaal Craton along the Thabazimbi–Murchison Lineament (TML; 2.7–3.0 Ga; Good and de Wit, 1997; Thomas et al., 1993);
- The Limpopo collisional event (ca. 2.7 Ga) took place during the late Archean consolidation of the Kaapvaal and Zimbabwe Cratons; tectonic activity continued in Paleoproterozoic. The Limpopo granulite–gneiss terrane of the Limpopo Mobile Belt (LB) contains a set of paleo-subduction systems with steeply dipping shear zones which separate tens of kilometer wide terranes (Barton et al., 2006); the axially symmetric belt is made of the Central Zone sandwiched between the Northern and Southern Marginal Zones which are ca. 50–100 km wide up-thrust deep-level granulite facies terranes of the adjacent cratons (McCour and Vearncombe, 1992; Smith et al., 2009);
- Ventersdorp intracontinental rifting (ca. 2.7 Ga) in the central part of the Kaapvaal Craton and the emplacement of flood basalts (Burke et al., 1985),
- the Olifants River Dyke Swarm (the oldest dated event is 2.5–2.9 Ga, followed by new events at 0.8–1.7 Ga), presently exposed in the northeastern Kaapvaal but probably substantially covered by sediments in the Witwatersrand Basin (Jourdan et al., 2006);
- Amalgamation of cratonic blocks, and final stabilization of the Kalahari Craton, accompanied by emplacement of granites at ~2.6 Ga (Rollinson, 1993); emplacement of the Great Dyke of Zimbabwe (2.575 Ga) — the last major tectono-thermal event that affected the Zimbabwe Craton (Jelsma and Dirks, 2002).

2.3. Paleoproterozoic tectono-magmatic events

- Intracratonic extension, formation of the Transvaal (2.2–2.6 Ga) and Waterberg (1.8–2.0 Ga) basins, and of the Magondi Basin at the western margin of the Zimbabwe Craton (ca. 2.0–2.2 Ga) (Thomas et al., 1993);
- Ventersdorp rifting II (2.05 Ga); magmatic rocks presently outcrop mostly within the Western Kaapvaal block but the inferred LIP extends over most of central Kaapvaal,
- Major subsidence of the Witwatersrand Basin (ca. 2.05 Ga), probably in response to the Ventersdorp LIP,
- The Vredefort impact event (2.023 Ga) which exposed the ca. 3.1 Ga old crust, probably down to the crust–mantle transition, in the central part of the Witwatersrand Basin (Lana et al., 2003),
- Emplacement of the intracratonic Bushveld Intrusion Complex (ca. 2.05 Ga) in the northern part of the Kaapvaal Craton; it may extend far beyond its outcrops and it is the largest known layered mafic intrusion in the world (Von Gruenewaldt et al., 1985);
- The Eburnian orogeny (ca. 2.0 Ga) along the western margin of the craton, amalgamation of the Kheis–Okwa and Magondi blocks to the craton. The Kheis orogeny (ca. 1.75 Ga) led to deformation and metamorphism of the Archean rocks along the western margin of the Kaapvaal Craton (Altermann and Halbich, 1991).

2.4. Mesoproterozoic and Pan-African tectonics

- The Kibaran orogeny (ca. 1.1–1.3 Ga) at the western and southern margins of the Kaapvaal; formation of the Namaqua and Natal metamorphic Provinces by juvenile arc-related, volcano-sedimentary sequences (0.9–1.3 Ga); amalgamation of the Rehobothian and the Namaqua–Natal lithospheric terranes; reactivation of the Kheis province (Thomas et al., 1993);
- Emplacement of the Umkondo continental flood basalts (ca. 1.1–1.2 Ga) which covered most of the Kalahari Craton; some of the oldest kimberlite magmatism in the Kaapvaal Craton (the Premier pipe),
- The Pan-African tectono-thermal event (ca. 500–600 Ma) related to the assembly of Gondwana which led to the formation of extensive intracratonic foreland basins; formation of the Damara orogen between the Kalahari and Congo Cratons and the Mozambique Belt along the eastern margin of the Kalahari Craton; refolding of the Magondi Belt;
- Orogeny at the Neoproterozoic Saldanian Province (the southwestern Cape Province) along the southern margin of the Namaqua–Natal Mobile Belt; a proposed associated subduction zone (or, alternatively, the Pan-African suture) is marked by the Beattie Magnetic Anomaly (De Beer, 1983).

2.5. Phanerozoic tectono-magmatic and orogenic events

- The Cape Fold Belt orogeny (ca. 280 Ma) as part of the assembly of Pangea; the orogen can be traced into South America, Australia, and Antarctica; some kimberlite magmatism in northern Kaapvaal, the Zimbabwe Craton, and the Limpopo Belt (0.2–0.6 Ga),
- Fragmentation of Gondwana; emplacement of the Karoo basalts (180 Ma) over most of southern Africa and Antarctica and associated emplacement of the Okavango, Save-Limpopo and Olifants River Dyke Swarms (180 Ma);
- Wide-spread kimberlite magmatism with a peak at ca. 90 Ma and continuing until ca. 50 Ma.

These plate tectonic events and plume-lithosphere thermo-chemical interactions which operated over a time span of almost 4 Gy resulted in the formation of an extremely complex crustal structure, highly heterogeneous in all parameters and at all scales.

3. Seismic data and processing

3.1. Seismic data

The Southern African Seismic Experiment (SASE) array extends NE–SW from the Cape Fold Belt in the SW to the central Zimbabwe Craton in the NE and crosses the Namaqua–Natal Mobile Belt, the core of the Kaapvaal Craton, and the Limpopo Belt, (Fig. 2). 55 broadband seismic stations acquired data for 2 years at 82 sites with roughly 100 km station interval. At the end of the first year, about half the stations were redeployed, such that the centrally located stations recorded for ca. two years, while the peripheral stations recorded for approximately one year.

The 3-component broadband instruments recorded teleseismic events with broad distributions of azimuth and distance (Fig. 3). We model seismic data from the entire array and seismic data available from three additional broadband digital stations of the Global Seismic Network (GSN). The current analysis is based on 6300 RFs from 220 events with magnitude ≥5.5 Mw at epicentral distances between 30° and 95°. These earthquakes provide a reasonably good distance and azimuth coverage (Fig. 3b).

We analyze the P-wave coda that contains considerable information about the crustal structures including converted S-waves generated at various depths below the seismic stations. The incident teleseismic rays are subvertically covering a conical-like volume beneath the stations such that the piercing points form a ring with 8–11 km diameter at the Moho interface around the perpendicular projection below the station (Fig. 3a).
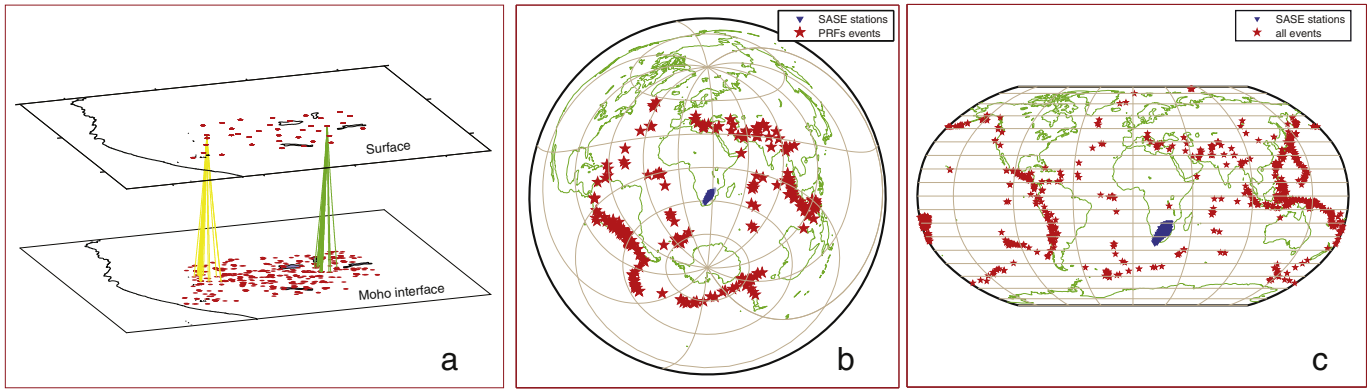
Fig. 3. a) Theoretical representation of the conical volume covered by the teleseismic incident rays, b) event distribution map used for PRF analysis, and c) distribution of all global events recorded by SASE which have been for selecting the PRF events.

3.2. Pds receiver functions

The principles of teleseismic conversion are described by classical geometrical-ray theory. Conversion at an interface between dissimilar materials occurs for both incident P- and S-waves with the partitioning of the energy between the different waves given by the Zoeppritz equations (Aki and Richard, 2002). The RF technique is designed to isolate the P to S conversions (Langston, 1979; Vinnik, 1977) by deconvolution of longitudinal components from horizontal components in either the time or frequency domain (Ammon, 1991; Dueker and Sheehan, 1998; Park and Levin, 2000; Poppeliers and Pavlis, 2003; Sheehan et al., 2000). On the assumption of an incident plane wave, the resulting waveform is an estimate of the impulse response at the stations as a function of slowness. With adequate distance coverage, RF can be used to determine the optimum depth of a discontinuity and the average velocity above it (Gurrola et al., 1994; Niu and Kawakatsu, 1998). The travel time difference, $\delta t_{(Pds-P)}$ between the Pds phase (converted from P to S at the discontinuity at a depth d beneath the receiver) and the direct P-wave, is a function of the depth and dip of a crustal discontinuity, the velocity structure (Vp and Vs) above the discontinuity, and the epicentral distance. $\delta t_{(Pds-P)}$ is available only at a single epicentral distance, therefore estimation of the depth d from $\delta t_{(Pds-P)}$ requires a reference velocity model and the determined depth is therefore model dependent. Alternatively the waveform of the receiver function can be inverted to extract an estimate of velocity structure and depth by exploiting all the reverberations and conversions (e.g., Shibutani et al., 1996).

Our RFs are calculated with the LQT method (Vinnik, 1977) in the version by Yuan et al. (1997). The method involves rotation of the geographically-oriented seismograms into ray coordinates. This decomposes the wavefield into subvertical (P), vertically-polarized shear (SV) and horizontally-polarized shear (SH) components. Following common procedure (Kumar et al., 2005; Li et al., 2007; Oreshin et al., 2002; Vinnik et al., 2004a, 2004b; Yuan et al., 1997), the P and SV components are assumed to be orthogonal and are determined by rotating the vertical and radial waveforms until the P-component amplitude at the mean converted S arrival time sample is minimized. All radial and transverse-component RFs are included in the analysis.

A straightforward frequency domain deconvolution can be unstable due to spectral holes in the vertical-component spectrum (Oldenburg, 1981). Stabilization of this process can be obtained by either "pre-whitening" (Robinson, 1954; Yilmaz, 1987) or "water-level" (Ammon, 1991; Clayton and Wiggins, 1976; Langston, 1979) algorithms. The former adds a small component of random noise to the vertical component, while the latter sets a lower bound on the magnitude of the denominator terms (the vertical seismogram spectral elements) in a frequency domain spectral division. In this study, converted phases are isolated by iterative, time-domain spiking deconvolution (Gurrola et al., 1995;

Ligorría and Ammon, 1999) with pre-whitening to stabilize the filtering. Pds phases are enhanced by stacking the deconvolved signals using the appropriate moveout corrections for different slowness (Yuan et al., 1997).

Iterative time domain deconvolution works well even with complex signals, but regardless of deconvolution algorithm, the response at the receiver depends on the complexity of structures. Simple structures generally lead to better RF images (Ligorría and Ammon, 1999). For this reason, the iterative real rotation angles (as compared to the model incidence angles derived from a standard velocity model such as IASP91) provide reasonable constraints at some sites of our study area. Some stations show noisy RFs if calculated using the model incidence angles; this may indicate complex crustal heterogeneity under some sites. We further filter the RF into two groups with band pass filtering of 1–20 s and 0.5–3.5 s before deconvolution which resolve different parts of the intra-crustal structure.

3.3. Hk-stacking

RFs include primary conversions and other coherent signals such as Moho reverberation phases, which are multiple reflections from the free surface and the Moho. RF studies have shown that one can estimate the average crustal Vp/Vs ratio (k) and simultaneously improve the determination of the Moho depth (H) by analyzing the arrival times of the converted and the reverberation phases (Niu and James, 2002; Zandt and Ammon, 1995; Zhu and Kanamori, 2000). This approach uses a model with a sharp single discontinuity at the base of the crust, and so performs less well where there is a gradational base to the crust as is common in Proterozoic terranes (see e.g., Kennett et al., 2011).

We carry out a grid search over the H–k space for determining the parameters that best explain the observed Moho conversion and its P and S multiples. We calculate the average values of H and k at each station, following the approach of Zhu and Kanamori (2000). The clear Moho multiples observed in much of the SASE seismic data result in well-constrained estimates of both crustal parameters. We determine the optimum H–k parameters by stacking the P_{SV}-RFs at each station along the travel time curves of the main converted and reflected phases at the Moho (Chevrot and van der Hilst, 2000). We test a series of candidate depths H_i in the range from 20 km to 70 km in increment of 0.1 km, and candidate k_j from 1.60 to 2.0 in increment of 0.0025. We calculate the moveout of Pds ($t_1^{(i,j)}$) using (Dueker and Sheehan, 1998; Sheriff and Geldart, 1993)

$$t_1^{(i,j)} = \int_{-H_i}^{0} \left[\left\{ \sqrt{\left(V_p(z)/k_j\right)^{-2} - p^2} \right\} - \left\{ \sqrt{V_p(z)^{-2} - p^2} \right\} \right] dz$$

where p is the P-wave ray parameter, H_i is the depth of the candidate discontinuity, k_j is the candidate apparent Vp/Vs, and $V_p(z)$ is the P-wave velocity at depth z. While the moveout, $t_2^{(i,j)}$ of Ppds can be calculated using

$$t_2^{(i,j)} = \int_{-H}^{0} \left[\left\{ \sqrt{\left(V_p(z)/k_j\right)^{-2} - p^2} \right\} + \left\{ \sqrt{V_p(z)^{-2} - p^2} \right\} \right] dz$$

and for Psds, $t_3^{(i,j)}$

$$t_3^{(i,j)} = \int_{-H}^{0} 2\sqrt{\left(V_p(z)/k_j\right)^{-2} - p^2}\, dz.$$

The RFs at each station are stacked using

$$A\left(H_i, k_j\right) = \sum_{k=1}^{n} w_1 S_k\left(t_1^{(i,j)}\right) + w_1 S_k\left(t_2^{(i,j)}\right) - w_1 S_k\left(t_3^{(i,j)}\right)$$

where n is the number of P_{SV}-RFs at the station, $S_k(t)$ is the amplitude of the point on the kth RF at time t after the first P arrival (where $t = t_1, t_2$ or t_3), and w_1, w_2, and w_3 are weighting factors that satisfy $w_1 + w_2 + w_2 = 1$ (Zhu and Kanamori, 2000). The optimal pair of (H_i, k_j) is the one that gives the maximum stacking amplitude, which is determined manually from a contour plot.

3.4. Moho sharpness and uncertainty

Moho depth estimation is largely dependent on the average crustal Vp and therefore uncertainties in the H values are generally of the order of 2 km (Kumar et al., 2002). Interpretation of seismic refraction profiles (Durrheim and Green, 1992) indicates insignificant variations in mean crustal velocity within a range of ±5%, which corresponds to an uncertainty of <3 km for the H estimation. Similarly, the small velocity variation has insignificant effects on the resulting k (Clarke and Silver, 1993; Zhu and Kanamori, 2000). Errors in average velocity transfer into errors in the H–k parameters. The chosen value for the average seismic velocity <Vp> was 6.5 km/s based on Durrheim and Green (1992) for southern Africa. Most of the events have epicentral distances >65° (Fig. 3b) which suggest that the rays arrive at the stations at near-vertical angles. Despite this fact, at some sites we observe significant changes in the RF patterns that may reflect small-scale heterogeneity in the crustal velocities. Changing the reference Vp by ±0.5 km/s, we find that H and k are perturbed with values of ±1 km and ±0.025, respectively.

A sharp transition at any discontinuity will produce strong converted and multiple phases. An abrupt velocity change at a discontinuity with little heterogeneity in the average velocity above it causes strong converted phases (the imaged crustal volume beneath the station has a cone-like shape with a maximum radius of ~10 km at the Moho, assuming an event at 30° epicentral distance). Short wavelength changes in crustal velocity will reduce the stacked amplitude of the main RF phases (Pds, Ppds and Psds) and increase the uncertainty of the estimated parameters. The amplitudes of the converted phases depend on the contrast of the P- and S-wave velocities across the discontinuity, which is usually the main cause of strong signals.

The sharpness of the Moho, i.e., its thickness and the contrast in velocity and density across the crust–mantle transition, affects the amplitude and frequency of the converted Pds phase and the expression of the multiples. A sharp Moho produces strong Pds and multiple phases with relatively short waveform. Other factors may also affect the amplitude of the converted phases, including lateral variation in Moho depth, significant short-wavelength variations in density and velocity around the Moho, and velocity heterogeneity in the crust in general and, in particular, in the shallow crust around the station. Variation in velocities

results in incoherent stacking and reduction in amplitude of the converted phases in stacked traces, whereas arrival time differences usually are smaller than the duration of the phases and therefore have limited effect on the stacked amplitude to instead affect the duration of the signal.

The sharpness of the Moho beneath a station can be quantified as the ratio between the stacked amplitude of the Pds phase, corresponding to the optimal pair of H and k, and the mean amplitude of the direct P wave on the SV components (Owens et al., 1984). In order to reduce the effects of the other factors discussed above, we modify the method to improve the compatibility of the phases by measuring the regional average of the Pds signal for the whole array and use this average value as the reference. Our measure of sharpness is therefore calculated as the amplitude of the Pds phase for each stacked trace beneath a station normalized with the average regional Pds amplitude. Where the crust–mantle transitional is gradational the Moho multiples are reduced in amplitude, and the Vp/Vs ratio for the whole crust tends to be less well defined. Hk-stacking will place the equivalent discontinuity near the middle of the gradient zone.

4. Depth to Moho in southern Africa

4.1. Present study

We calculate 1-D RF stacks for the entire array (Fig. 4, see also Fig. S5) after moveout correction based on Hk-stacking analysis. The Pds conversion from the Moho is the dominant signal on most of the depth images. Relatively thin crust and very sharp, well-defined Pds conversions are typical for most of the Kaapvaal and Zimbabwe Cratons and the northern and southern margins of Limpopo Belt. Pds arrivals from the Moho associated with the Bushveld Complex of the Kaapvaal Craton and the surrounding post-Archean terranes (Kheis, Okwa, Namaqua–Natal and Cape Fold Belts) of the craton are all diffuse and have relatively small amplitude.

Band pass filtering shows that the RF images are strongly frequency-dependent through the cratonic regions of Kaapvaal, Zimbabwe and the marginal parts of Limpopo. Low-frequency (1–20 s) RFs show a relatively homogeneous crust with a sharp Moho (Fig. 5a), whereas high-frequency (0.5–3.5 s) RFs show a clear mid-crustal discontinuity (MCD) in addition to the Moho conversion (Fig. 5b).

The presence of this frequency dependence indicates structural complexity which may include anisotropy. Crustal anisotropy on the RFs signals is indicated by phase reversal of the 1–20 s P_{SV}- and P_{SH}-RFs at each station for the MCD and Moho phases through a 2π backazimuth cycle. The anisotropy effects cause an observed polarity reversal of the Pds, which tends to weaken the energy of, in particular, the stacked P_{SH}-RFs. For this particular case, we have therefore chosen to stack only positive signals. This feature will be the topic of additional studies (Youssof et al., in preparation). We also find that the extreme crustal heterogeneity at some sites may lead to misinterpretation if the theoretical ray parameters are used for calculating the RFs. At these stations, we compare the results based on model and real ray parameters. Due to crustal heterogeneity, some stations show noisy RFs if calculated using the model incidence angles. This is illustrated, for instance, by station SA75 of Zimbabwe Craton (Fig. 6) where the P_{SV}-RFs were calculated using both observational and theoretical ray parameters. In the LQT approach the P-wave contribution at zero-time should be suppressed when the appropriate slowness is used. The improvement with empirical incidence angles is clearly observed on the zero-time arrival as well as in the clarity of the Pds arrivals of the Moho and MCD convertors.

Our results indicate a highly heterogeneous structure of the crust with short wavelength variations in thickness (Fig. 7a, see also Fig. S1a) and intra-crustal structures (Fig. 5, see also Tables 1 and S1 for details). The stacked RFs image a sharp Moho transition between 4 and 5 s in the cratonic blocks of Kaapvaal and Zimbabwe as well as the marginal borders of Limpopo, which is consistent with previous observations
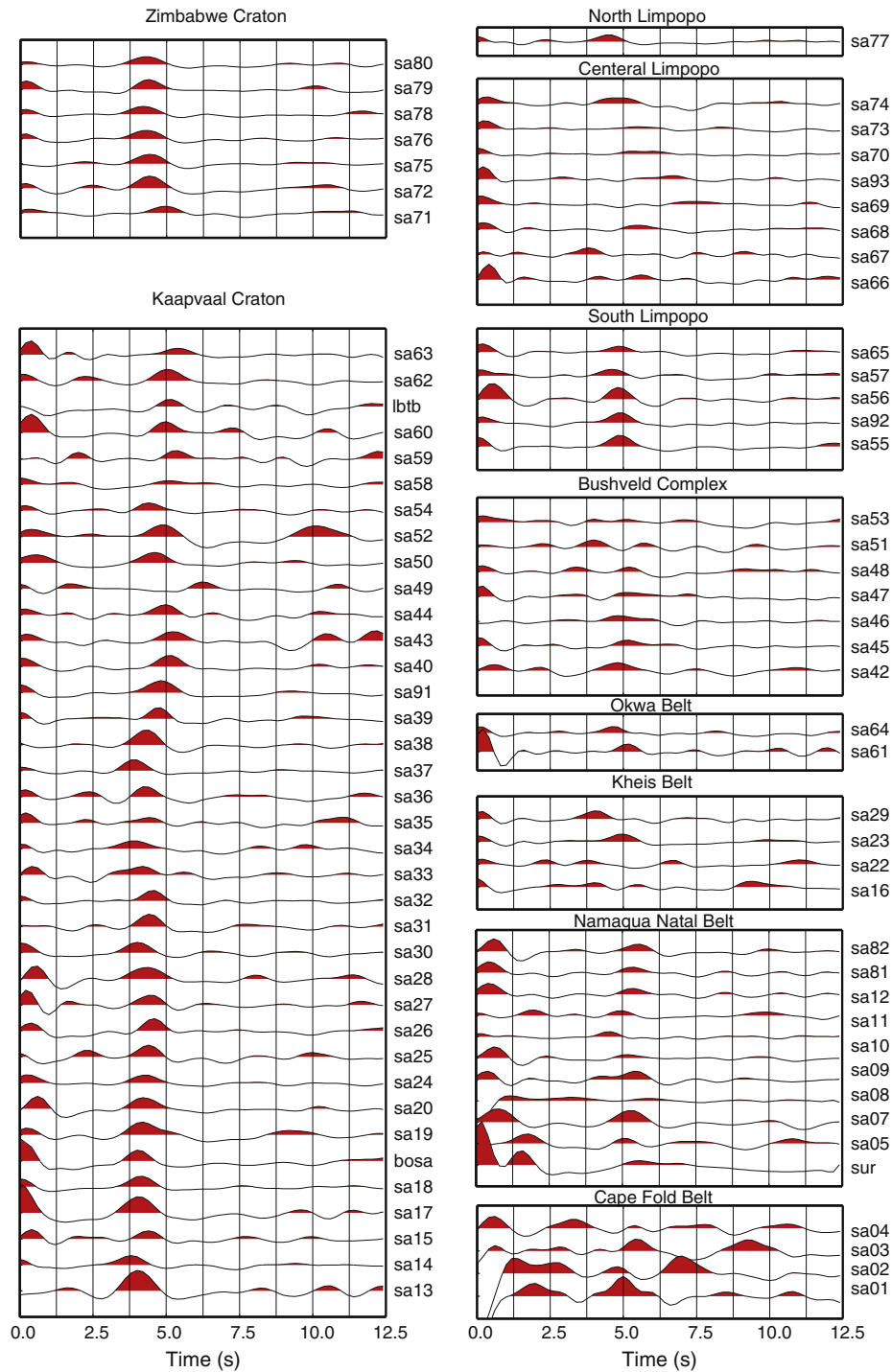
Fig. 4. One-dimensional RF stacks for the entire array organized by geologic province. The station name is shown to the right of each trace. Pds arrivals in modified regions of the craton and post-Archean terranes tend to be more diffuse and of smaller amplitudes than in cratonic areas. See Supplementary Fig. S5 for the stacked RFs with longer time window.

(James et al., 2003; Nguuri et al., 2001; Niu and James, 2002). A new observation is the strong Pds phases from the top of the lower crust. This phase is weak in the broadband RF but clearly observable in the high frequency RF. It is most pronounced in the Kaapvaal Craton with arrival times between 1.7 and 2.5 s, and is weak in the Limpopo Belt with arrival times of 2.2 to 2.8 s, whereas it is barely observable in the Zimbabwe Craton (Fig. 5b). The Pds Moho signals in the mobile belts of Kheiss, Okwa, Namaqua–Natal and Cape Fold around the Kaapvaal Craton are scattered and have smaller amplitudes than in the Kaapvaal and Zimbabwe Cratons. Our use of the Hk-stacking for all stations (Fig. S4) provides reliable

estimates of Moho depth and Vp/Vs ratio throughout the area. New results are the identification of significant short wavelength variations in Moho depth and Vp/Vs ratio, which indicate a heterogeneous crust at smaller scale than indicated by earlier studies.

The RFs observed in this study have mapped the Moho depths with the following trends over southern Africa (Fig. 7a):

- the Archean crust of central and southern Kaapvaal has crustal thicknesses of 34–44 km in western block (Ventersdorp LIP) and 36–44 km in eastern block (Witwatersrand Basin), with a pronounced
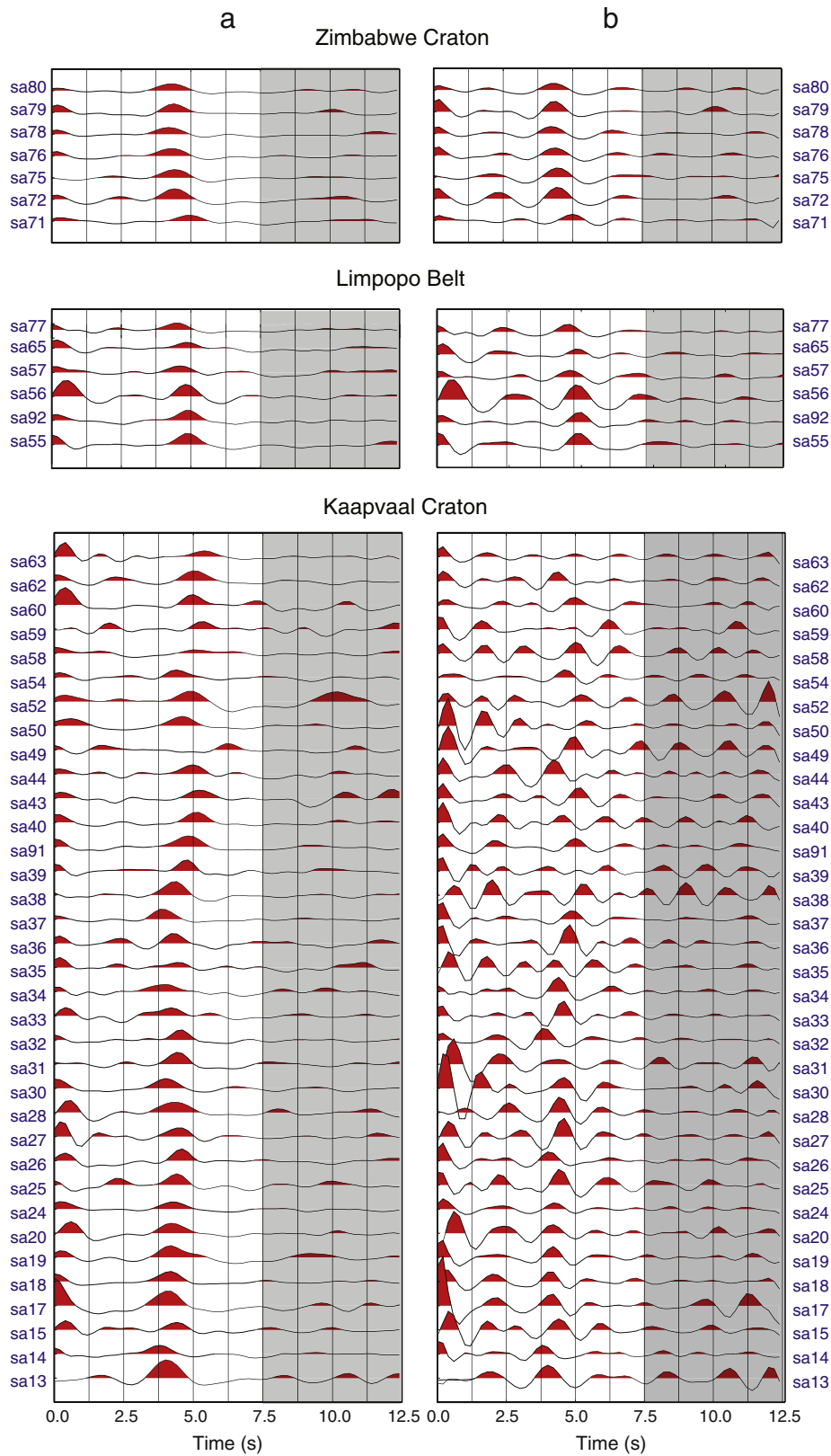
Fig. 5. One-dimensional RF stacks for the Archean areas of the Kaapvaal, Zimbabwe Cratons and the Limpopo Belt. Traces are sorted by station number. The station name is shown beside each trace. Band-pass filters have been applied before deconvolution with cut-off frequencies: a) 1–20 s and b) 0.5–3.5 s. Individual RFs have been corrected for move-out before stacking; for some stations where anisotropy or heterogeneity cause phase reversals, only the positive amplitudes have been used for the stack. The high frequency RFs show significant amplitudes of the mid-crustal discontinuity. The Pds conversion from the Moho is the dominant signal on most of the depth images shown. Relatively thin crust and sharp, well-defined Pds Moho conversions are associated with the south-central Kaapvaal Craton.
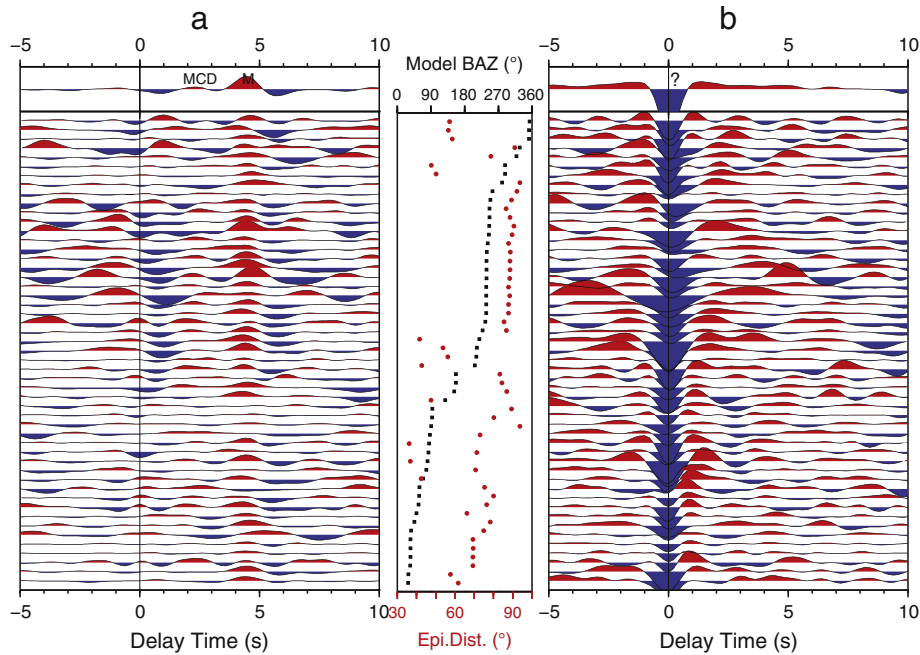
Fig. 6. P$_{SV}$-RFs of station SA75 calculated a) using real incidence angles and b) assuming theoretical angles. The figure illustrates the improvement achieved from using real instead of theoretical angles where artifacts are generated by complex crustal velocity structure that significantly deviate from the assumed reference model.

local minimum (34 km) at the Vredefort impact structure. Although this part of southern Africa has been termed as "undisturbed" crust (James et al., 2003), we note that the Archean crust of this area has been affected by a number of tectono-magmatic events, such as the Ventersdrop rifting and associated basin subsidence;

- the Moho is deep (45–50 km) in the center between the two surface exposures (lobe-like shape) of mafic intrusion of the Bushveld Intrusive Complex (BIC). This complex is characterized by enormous magma intrusions, which form the largest mafic body in the world with an estimated intrusive volume of over 1 million km^3 (Cawthorn and Walraven, 1998). Remarkably the Moho depth is smaller than in the central part of the complex, 46–49 km below the eastern lobe and 42–45 below the western lobe of the intrusion;
- the oldest terranes, located in Swaziland in NE Kaapvaal, have a Moho depth of 44–49 km; this belt of thick crust may be linked to the Bushveld Intrusive Complex;
- some of the oldest terranes (the Pietersburg–Giyani–Murchison (PGM) block between Thabazimbi–Murchison Lineament (TML) and the Limpopo Belt) have a relatively uniform crustal thickness of 34–39 km, very similar to Western Kaapvaal; the TML marks a sharp change in crustal structure from a thin Kaapvaal crust to a thick Limpopo crust;
- most of the central zone of the Limpopo Belt (LB) has a relatively uniform crustal thickness of 41–46 km, whereas it is only 40–42 km in the marginal zones and 35 km at the eastern end of the LB;
- crustal thickness in the Tokwe block of the southern Zimbabwe Craton is 35–38 km, which is similar to Western Kaapvaal, and 47–51 km in the Tati block at the western margin of the craton (affected by the Okavango Dyke Swarm);
- most of the Namaqua–Natal (NNMB) and parts of the Cape Fold Belts (CFB) have a relatively uniform crustal thickness of 45–48 km with some local anomalies (41–42 km in NNMB and ca. 34 km in West CFB).

In summary, the Archean cores of both the Kaapvaal and the Zimbabwe Cratons have crustal thicknesses of 35–40 km, whereas tectonic segments that have undergone compressional events, regardless of age (LB, NNMB), and the Bushveld Intrusive Complex (BIC) have crustal thicknesses of ca. 45–50 km. The Archean cores of both cratons show sharp Moho conversions (Pds) with strong P and S multiples (Ppds and Psds) and clear conversions from an intra-crustal boundary.

We have assessed the sharpness of the Pds waveform from the Moho based on the following criteria: a sharp Moho is characterized by high amplitude and short duration of the signal, whereas a gradual Moho is characterized by small amplitude and long signal duration. Similar analysis has earlier been successfully applied to data from controlled source seismology (Jensen and Thybo, 2002; Thybo et al., 1998), where the Moho variability is related to magmatism and underplating in relation to basin formation.

The resulting map (Fig. 8, see also Fig. S3) shows that a sharp Moho is observed in thin crust with relatively small Vp/Vs in most of the Archean Zimbabwe and Kaapvaal cratons, and a gradual Moho is observed in thick crust at the Okavango Dyke Swarm, the Namaqua–Natal Mobile Belt and in the central and western parts of the Bushveld Intrusive Complex. We discuss tectonic implications of the Moho sharpness in Section 6.

4.2. Other regional crustal seismic models

Seismic reflection and refraction profiles image a slow and thin crust in the Witwatersrand Basin in the central and eastern Kaapvaal Craton and in the Namaqua–Natal Belt (de Wit and Tinker, 2004; Durrheim and Green, 1992; Green and Durrheim, 1990). Durrheim and Green (1992) conclude from a refraction study that 1) the Archean Kaapvaal has an average Moho depth of about 35 km with a slight positive velocity gradient beneath the Moho, 2) the crustal thickness ranges from about 30 km in the center of LB to 40 km within the Zimbabwe Craton, 3) NNMB has a Moho depth of 42 km and 4) the CFB has an average crustal thickness of 33 km. The interpretation of traveltimes of Witwatersrand mine tremors observed on a profile across the LB has revealed Moho depths between 30 and 35 km (Durrheim et al., 1992). These active source experiments are limited in coverage. Our results (Moho depths of 33–39 km) are generally in agreement with the active source results, in the core of Kaapvaal (Witwatersrand). However, the RF model indicates a significantly deeper Moho than the refraction model in the LB, NNMB and CFB.

A number of RF and tomography studies based on the SASE data (e.g., James et al., 2003; Kwadiba et al., 2003; Nair et al., 2006; Niu and James, 2002) generally agree in estimating the Moho at around 35–
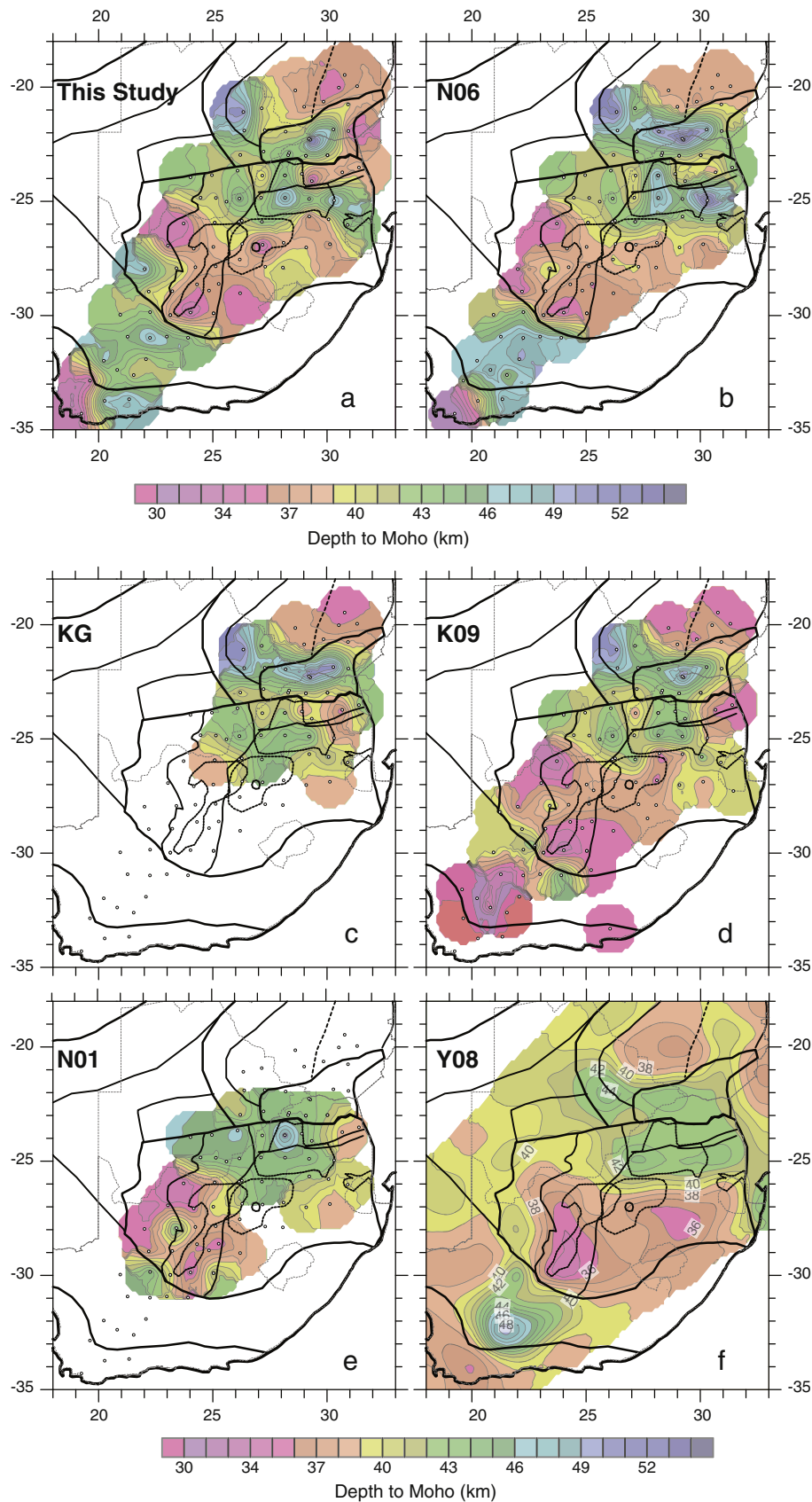
Fig. 7. Comparison of different models of Moho depth in southern Africa based on SASE array data. Tectonic boundaries as in Fig. 1. See Supplementary Fig. S1 for the same maps with values inserted at each station. (a) This study based on P-RF, the corresponding Vp/Vs values are shown in Fig. 9a; (b) P-RF model of Nair et al. (2006), the corresponding modelled Vp/Vs values are shown in Fig. 9b for 44 stations; (c) model of Kgaswane et al. (2012) for the northern Kaapvaal around the Bushveld Intrusion Complex based on teleseismic P-RF and 2–60 s period Rayleigh wave group velocities merged with the model of Gore et al. (2009) for the Limpopo Belt and Zimbabwe Craton based on P-RF and adopting Vp/Vs = 1.75 for this region; (d) model of Kgaswane et al. (2009) based on joint inversion of P-RF and 10–175 s period Rayleigh wave group velocities dispersion curves; (e) P-RF model of Nguuri et al. (2001) assuming constant Vp/Vs = 1.73; (f) model of Yang et al. (2008) based on ambient noise and teleseismic tomography (Rayleigh wave phase velocities at periods of 6 to 143 s).

40 km depth in the Kaapvaal Craton (Fig. 7). Moho depth estimations, based on RFs calculated for 35 teleseismic events for 79 stations, assuming Vp/Vs = 1.73 everywhere (Nguuri et al., 2001), are in agreement with our results for the Archean cratonic core (Fig. 7e), where the observed Vp/Vs is close to 1.73 (Fig. 9a). However, where the Vp/Vs ratio deviates from 1.73 in crustal blocks that have undergone significant geodynamic reworking, there is a significant difference from the earlier results y (Fig. 7a and e).

Niu and James (2002) use crustal reverberations to estimate the velocity and density jump across the Moho and to determine Poisson's ratio at a 60 km × 40 km area of the crust at KTA (near station SA19). Their analysis of waveform broadening indicates a thickness of the Moho transition zone of less than 0.5 km and a maximum variation in crustal thickness over the KTA region of less than 1 km. In agreement with our results on the Moho depth and Vp/Vs ratio, the flat and almost perfectly sharp Moho at a depth of 34.5 km and low average crustal Poisson ratio of ~0.254 indicates absence of a mafic lower crust. Local mining events recorded by the same array were used to model waveforms (James et al., 2003). Beneath Kimberly, the average P-wave velocity is determined to be 6.46 km/s, which results in an average S-wave velocity of 3.71 km/s for the crust using a modified IASP91 crustal model. The estimated crustal thickness from the lapse time of Pds is 35.4 ± 0.2 km, in a very good agreement with our and previous results from RF as well as refraction studies of that location surrounding Kimberly (Durrheim and Green, 1992).

The first analysis of almost all of the SASE data (Nair et al., 2006) calculated 1445 radial RFs from 88 teleseismic events to determine the spatial variations in Moho depth for 72 SASE and 3 permanent stations (Fig. 7b). These authors analyzed 44 stations with clear Pds, Ppds and Psds phases by Hk-stacking, but for the remaining 34 stations, they estimate H by assuming k = 1.73. Similar to the results of Niu and James (2002), the Moho depth estimates are similar to the present study for the stations where Hk-stacking was used and where the assumed k = 1.73 is representative of the true crustal structure.

Based on 89 stations from both SASE and the Africa Array network, joint inversion of RFs and Rayleigh wave group velocities (Kgaswane et al., 2009) led to Moho depth estimates comparable to previous results, except for 9 stations (SA05, SA09, SA49, SA81, SUR, SA16, SA47, SA48, SA70) where their results deviate by more than ± 5 km from the RF results. Here the velocity profiles show complicated lower crustal structure, commonly with a gradational Moho. Our results show a more than 5 km deeper Moho for the NNMB, Kheiss and CFB than the results by Kgaswane et al. (2009) but are in agreement for the cratonic core where the difference between the two results is in average within ± 2 km. Our deeper Moho estimate may arise from the positioning of an equivalent discontinuity within the gradient zone. In sharp contrast to other studies, Kgaswane et al. (2009) reported a surprisingly thin crust in most of the NNMB (Fig. 7d) where their Moho depth corresponds our interpretation of the mid-crustal discontinuity (MCD).

Gore et al. (2009) find a crustal thickness of 42–53 km with a complex Moho in the LB, and 36–39 km in the Zimbabwe Craton with a relatively sharp and simple Moho and no apparent mid-crustal discontinuities. Joint inversion of high-frequency teleseismic RFs and 2–60 s period Rayleigh wave group velocities for 16 broadband seismic stations reveal deep Moho (a maximum depth of 45 km) in the center of the Bushveld Intrusion Complex (BIC) with a high velocity (Vs ≥ 4.0 km/s) lowermost crust (Kgaswane et al., 2012). For most of the stations, the thickness of this layer exceeds 5 km, but for a few stations (e.g., station SA50), it is less. Moho depth is similar in our model in the BIC while for the 7 stations outside of BIC it is 2 km deeper (Fig. 7a and c). The presence of the fast lowermost crust may be associated with magmatic underplating.

Pn tomography based on 1337 arrivals from 60 mining-induced tremors constrains the Moho depth at 46 stations in the Kaapvaal Craton, assuming a uniform upper mantle wavespeed across the entire region (Kwadiba et al., 2003). The estimated Moho depth within the

southern part of the craton is between 31 and 56 km, (average of 38.1 ± 0.9 km). These results differ from our RF model between + 12.4 km at SA37 and − 7.3 km at SA17. Moho depth is in the northern part of the craton between 41 and 59 km, (average of 50.5 ± 0.9 km) for 19 other stations. This is significantly deeper at all stations except SA40 than our model, (maximum + 18 km difference). They argue that differences between the Pn and RFs results are due to variable seismic properties of mafic granulites in the underplated northern part of the craton, which results in lack of a clearly defined Moho in the RFs. However, we have not observed the signal after the Pds phase that could indicate a weak transition.

Wright et al. (2004) refine the study of Kwadiba et al. (2003). They conclude that the refracted arrivals from the mantle (Pn and Sn) indicate a crustal thickness of ca. 50 km in the northern part and ca. 38 km in the southern part of the Kaapvaal Craton, where the RFs estimates are 43.6 ± 0.6 km and 37.6 ± 0.7 km. Wright et al. (2004) argue that the estimates from RFs in the north may be caused by variations in composition and metamorphic grade in an underplated, mafic lower crust, resulting in a crust–mantle boundary that yields weak P-to-SV conversions (Wright et al. (2004)). We do not observe evidence for such assumption in the RFs.

Ambient noise tomography for Rayleigh wave phase velocity maps at periods from 6 to 40 s (Yang et al. (2008)) indicates the same trends in regional crustal thickness variations as most of our study, with a relatively thin crust in the Kaapvaal and Zimbabwe Cratons (ca. 37 km) and thick crust (ca. 43 km) in the mobile belts (Fig. 7f). This ambient noise result shows a variable Moho topography in southern Africa. But the details do not always agree. Their study indicates that the structural variations in the upper crust tend to be anticorrelated with those in the middle and lower crusts, especially in the Kaapvaal Craton and the NNMB. Additionally, a very large velocity jump (from ~3.8 to 4.6 km/s) across the Moho is determined in the entire region.

5. Vp/Vs ratio and crustal composition

5.1. Present study

Vp/Vs ratios in crustal rocks are sensitive to rock composition and generally increase with higher mafic contents (Holbrook et al., 1992; Zandt and Ammon, 1995). In this section, we present our results that indicate a highly heterogeneous composition of the crust with short wavelength variations as reflected by the Vp/Vs ratio (Tables 1 and S1). Our Vp/Vs results are most reliable in the regions with a relatively sharp Moho, i.e., red zones in Fig. 8.

The crustal composition has the following patterns over the area (Fig. 9a, see also Fig. S2a):

- The Archean crust of central and southern Kaapvaal largely has values less than 1.73. Western Kaapvaal (Ventersdorp LIP) has the lowest Vp/Vs ratio of 1.67–1.73, which is surprising since one would expect that a LIP should include magmatic underplating and, therefore, high Vp/Vs. However, we cannot exclude that the RFs cannot distinguish a high-velocity lower crust from the uppermost mantle, such that the Moho has been misplaced at the top of the lower crust. Similar misinterpretation has been made in Greenland (cf. Artemieva and Thybo, 2008; Artemieva et al., 2006; Dahl-Jensen et al., 2003; Kumar et al., 2007; Thybo and Artemieva, 2013). Another possibility is that the lower crust has been metamorphosed into eclogite facies and now either has seismic velocity like the mantle or has been delaminated due to higher density (Griffin and O'Reilly, 1987; Mengel and Kern, 1992);
- Eastern Kaapvaal (Witwatersrand Basin) has high Vp/Vs of 1.75–1.76, with a local maximum of 1.80 associated with the Vredefort impact structure. Basin subsidence may be caused by density increase related to the LIP, but given that the major Ventersdorp rift is located further west, the underplating and possible eclogitization might have been less intense in eastern than western Kaapvaal;

Table 1
Results of receiver function analysis for the entire SASE array.

Station	Lon.	Lat.	Moho Depth	Apparent Vp/Vs	Poisson ratio	Moho sharpness
Zimbabwe						
SA72	28.61	−20.14	38	1.74	0.253	3.5
SA75	29	−20.86	37	1.9	0.308	1.2
SA76	29.85	−20.64	36	1.75	0.258	2.3
SA78	30.77	−19.47	36.5	1.74	0.253	2.2
SA79	30.52	−20.02	35	1.79	0.273	2.7
SA80	31.32	−19.96	37	1.75	0.258	2.2
W Zimbabwe						
SA66	26.37	−21.9	46.5	1.77	0.266	1.2
SA67	27.27	−21.89	39.5	1.79	0.273	1.7
SA70	26.34	−21.09	50.5	1.75	0.258	0.7
SA71	27.14	−20.93	40.5	1.8	0.277	2.0
Limpopo Belt						
SA55	28.3	−22.98	44.5	1.7	0.235	2.8
SA155/SA92	28.34	−22.88	44.5	1.7	0.235	2.6
SA56	29.07	−23.01	42.5	1.74	0.253	3.0
SA57	30.02	−22.98	41.5	1.72	0.245	1.6
SA65	27.22	−22.82	43	1.74	0.253	1.6
SA68	28.19	−21.95	41	1.87	0.300	1.0
SA69	29.27	−22.31	54.5	1.94	0.319	0.7
SA169/SA93	29.21	−22.26	43	1.74	0.253	0.9
SA73	30.28	−21.85	46	1.79	0.273	0.5
SA74	30.94	−21.92	34.5	1.93	0.317	1.5
SA77	30.92	−20.76	39.5	1.72	0.245	1.8
N. Kaapvaal (Bushveld Complex, Barberton Greenstone Belt, Pietersburg–Giyani–Murchison block)						
SA42	29.22	−25.67	36	1.84	0.290	2.1
SA43	30.07	−25.79	39	1.83	0.287	1.5
SA44	30.9	−26.03	44	1.72	0.245	1.5
SA46	27.11	−24.84	41.5	1.74	0.253	1.5
SA47	28.16	−24.85	49.5	1.7	0.235	1.0
SA48	29.22	−24.9	45.5	1.74	0.253	1.2
SA49	30.31	−24.96	48.5	1.83	0.287	1.1
SA51	28.16	−23.86	45	1.68	0.226	1.0
SA52	28.9	−23.8	39.5	1.74	0.253	1.9
SA53	29.33	−24.11	33.5	1.74	0.253	0.7
SA54	30.67	−23.73	37	1.74	0.253	1.4
SA58	31.4	−23.52	38.5	1.84	0.290	1.4
NW Kaapvaal (Gaborone Granites)						
SA45	26.16	−24.88	46	1.75	0.258	1.5
SA50	27.17	−23.87	39	1.74	0.253	2.1
SA59	24.46	−24.84	41.5	1.78	0.269	1.9
SA60	24.96	−23.85	41.5	1.77	0.266	2.3
SA62	25.14	−24.85	40.5	1.8	0.277	2.4
SA63	26.08	−23.66	43	1.79	0.273	1.7
E. Kaapvaal (Witwatersrand Basin)						
SA26	26.18	−27.55	38.5	1.76	0.262	2.4
SA32	26.29	−26.87	39	1.75	0.258	3.1
SA33	27.18	−26.9	33.5	1.8	0.277	2.3
SA34	28.1	−26.81	38	1.72	0.245	1.1
SA40	27.15	−25.9	43.5	1.78	0.269	2.2
W. Kaapvaal (Ventersdorp LIP)						
SA13	23.14	−29.98	36.5	1.71	0.240	2.8
SA14	24.02	−29.87	33.5	1.74	0.253	2.2
SA15	25.03	−29.9	36.5	1.76	0.262	2.3
SA18	24.31	−28.63	36	1.73	0.249	2.6
SA19	24.83	−28.91	36.5	1.7	0.235	3.5
SA24	24.24	−27.88	38	1.73	0.249	2.1
SA25	25.13	−27.85	37.5	1.76	0.262	2.8
SA30	24.17	−27.07	36.5	1.71	0.240	3.0
SA31	25.02	−27	38.5	1.73	0.249	3.0
SA37	23.72	−25.97	34	1.74	0.253	2.8
SA38	25.09	−25.93	39.5	1.69	0.231	2.3
SA39	26.15	−25.9	41.5	1.75	0.258	2.7
SA139/SA91	26.27	−25.85	41	1.76	0.262	2.3
SE Kaapvaal						
SA20	26.2	−29.02	35	1.76	0.262	2.6
SA27	27.29	−27.86	39	1.71	0.240	2.2
SA28	28.07	−27.9	41	1.74	0.253	3.0
SA35	29.09	−27.02	39	1.73	0.249	1.5
SA36	30.13	−26.88	36.5	1.75	0.258	1.9

Table 1 (*continued*)

Station	Lon.	Lat.	Moho Depth	Apparent Vp/Vs	Poisson ratio	Moho sharpness
Kheis–Okwa Mobile Belt						
SA16	22.2	−28.95	40	1.66	0.215	0.6
SA17	23.23	−28.93	38.5	1.67	0.220	2.9
SA22	22.01	−27.97	48	1.91	0.311	1.0
SA23	23.41	−27.93	41.5	1.77	0.266	2.0
SA29	23.04	−26.93	35	1.75	0.258	2.1
SA61	24.02	−23.95	43.5	1.76	0.262	2.0
SA64	26.2	−22.97	41	1.75	0.258	1.6
Namaqua–Natal Mobile Belt (NNMB)						
SA05	21.54	−32.61	42	1.77	0.266	1.5
SA07	20.23	−31.98	46.5	1.71	0.240	3.1
SA08	22.07	−31.91	41.5	1.95	0.322	0.7
SA09	22.99	−30.92	46	1.75	0.258	2.2
SA10	23.91	−30.97	44.5	1.74	0.253	0.9
SA11	20.95	−29.97	42	1.69	0.231	1.6
SA12	22.25	−29.85	43	1.76	0.262	1.3
SA81	21.27	−30.93	45	1.78	0.269	1.5
SA82	22.25	−30.98	48	1.75	0.258	2.0
Cape Fold Belt (CFB)						
SA01	19.25	−34.29	33.5	1.79	0.273	3.3
SA02	20.27	−33.74	47	1.92	0.314	1.8
SA03	21.34	−33.66	48	1.6	0.179	3.0
SA04	19.62	−32.85	34	1.62	0.192	0.7

- a marked minimum of 1.68 is observed in the central Bushveld Complex, where otherwise the Vp/Vs values are 1.7–1.74, and 1.83 at the easternmost branch of the intrusion, indicative of the presence of a large volume of mafic material. The variations in Vp/Vs indicate that the two branches of the intrusions, as observed at the surface, may not be connected at depth as otherwise interpreted from gravity (Webb et al., 2004);
- the NW block of the Kaapvaal Craton (Gaborone granites) which has not been affected by Ventersdorp LIP, has high Vp/Vs = 1.77–1.80; this may be related to the Eburnian orogeny (ca. 2.0 Ga) along the

western margin of the craton which led to deformation and metamorphism of the Archean rocks along the western margin of the Kaapvaal Craton;
- the oldest Swaziland terrane in NE Kaapvaal has Vp/Vs = 1.72 (1 station only);
- the Pietersburg–Giyani–Murchison (PGM) block between TML and LB has a relatively uniform ratio of 1.74;
- a pronounced anomaly with the highest Vp/Vs values in the region co-incides with the Olifants River Dyke Swarm in northeastern Kaapvaal (Vp/Vs ~ 1.83) and the Save-Lebombo Dyke Swarm in the Limpopo Belt/southern Zimbabwe Craton (Vp/Vs ~ 1.87–1.93). The high Vp/Vs anomaly (1.87–1.90) in the southern Zimbabwe Craton is apparently associated with the intersection ("triple junction") of the Okavango and Save-Lebombo dyke swarms where high Vp/Vs may be caused by magmatic intrusions into the crust;
- the western and southern Limpopo Belt has relatively low Vp/Vs, 1.72–1.74, similar to Western Kaapvaal;
- the Vp/Vs in the Tokwe block of the southern Zimbabwe Craton is significantly higher than in Western Kaapvaal, 1.75–1.79; similar values are observed in the Tati block at the western margin of Zimbabwe Craton; one may argue that this block represents an "undisturbed" Archean crust, whereas the lower crust may be lost in the Ventersdorp segment;

the Namaqua–Natal and the Cape Fold Belts are highly heterogeneous with typical values of Vp/Vs = 1.74–1.78 in NNMB.

Our Hk-stacking analysis shows that the average Vp/Vs of the crust for the entire area is 1.76. For the cratonic region, excluding the mobile belts, average crustal values are k = 1.75 (σ = 0.257) and Vs = 3.68 km/s. These values are in contrast to the assumed Vp/Vs ratio of 1.73 used in previous RF studies (Nair et al., 2006; Nguuri et al., 2001). The Vp/Vs ratios overall correlate with tectonic structures; the crust of the Ventersdorp LIP, the center of BIC (both in the Kaapvaal) and the northern LP tends to have low Vp/Vs (1.68–1.74), whereas regions affected by dyke-swarm magmatism have very high Vp/Vs (1.85–1.93).

5.2. Other regional crustal seismic models

The velocity and density jump across the Moho and the Poisson's ratio of the crust at Kimberley (southern Kaapvaal) was analyzed by Niu and James (2002) RF waveform. They find a density of the lowermost crust of 2.86 g/cm³, indicating rocks of felsic to intermediate composition, a density contrast across the Moho of 15.4 ± 2.3%, and
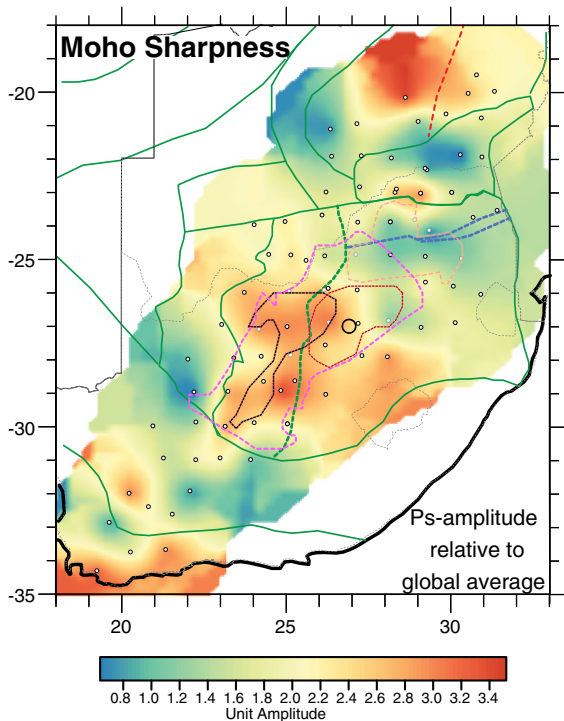

Fig. 8. Map illustrating the sharpness of the Moho transition determined as the amplitude of the Pds phases relative to the average Pds amplitude in the study area. Large values correspond to a sharp Moho transition (a strong converter). Tectonic boundaries as in Fig. 1. See Supplementary Fig. S3 for the same map with Vp/Vs values inserted at each station.
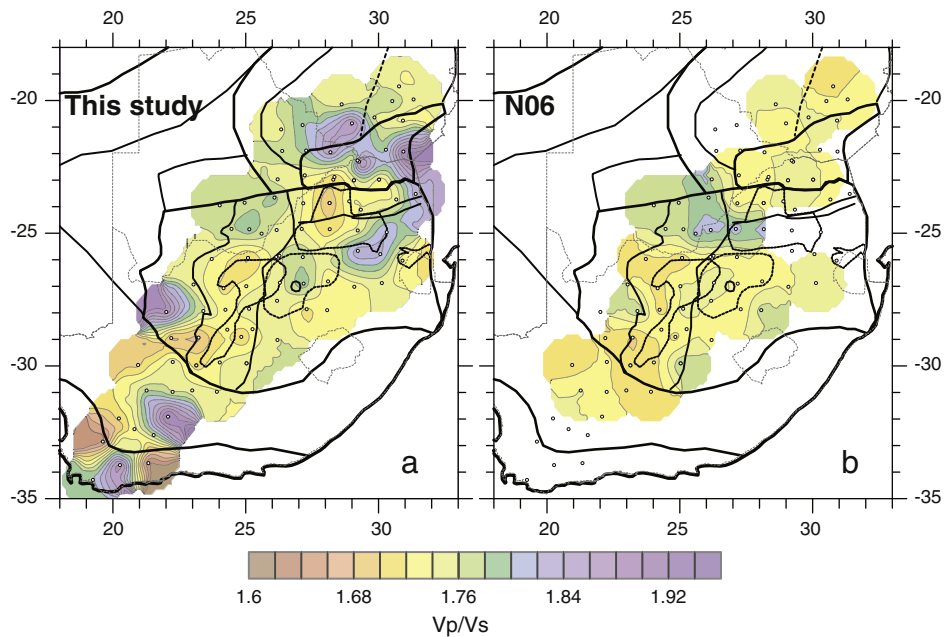
Fig. 9. Average crustal Vp/Vs ratio based on RFs analysis: (a) present study for the entire SASE array; and (b) model of Nair et al. (2006) for 44 stations. Tectonic boundaries as in Fig. 1. See Supplementary Fig. S2 for the same map with Vp/Vs values inserted at each station.

an S-wave velocity jump across the Moho of 17.3 ± 2.2%. This is a minimum estimate since any lateral heterogeneity of velocity within the crust or any lateral variation of Moho depth will produce phase shifts of Pds that degrade the amplitude of the stacked Pds waveform. The resulting average Vp/Vs ratio of the crust beneath the array is 1.742 ± 0.007, whereas we find 1.70 at station SA19. However, we reach almost the same range by averaging the 6 stations around SA19.

Nair et al. (2006) find that Vp/Vs ratios in the Kaapvaal Craton are on average less than 1.73 although 1.77–1.82 in the northern part of the cra- ton, including the western BIC (Fig. 9b). Similar Vp/Vs ratio of 1.8 was found for northern Kaapvaal based on seismic refraction modeling (Durrheim and Green, 1992), and was interpreted by the presence of hy- drated rocks. Our results indicate that the average Vp/Vs is less than of 1.75 in northern Kaapvaal including BIC. Relatively low Vp/Vs in central Kaapvaal is interpreted by felsic composition of the Archean crust separat- ed from the mantle by a sharp Moho. According to Gore et al. (2009), Poisson's ratio indicates a relatively more mafic crust (Vp/Vs > 1.76) in the LB than in the Achaean Zimbabwe Craton (Vp/Vs ≤ 1.76), which is in agreement with our finding of 1.75 within the Archean area and 1.79 outside.

6. Crustal structure and tectonic evolution

6.1. Cratons of Southern Africa

We discuss the heterogeneity of crustal thickness and composition in the context of the tectono-magmatic evolution of southern Africa since the Archean, based on our results for the Vp/Vs ratio, the Moho depth and Moho sharpness (Table 1), which indicate a complex mosaic of crustal blocks with significant short-wavelength variations in crustal structure, that do not always follow terrane boundaries established from surface geology. For this reason, we subdivide the area into crustal blocks based on the similarity of the Vp/Vs ratio and the Moho depth (Figs. 7a and 9a). To simplify the following discussion, the newly recog- nized crustal blocks are labeled by tectonic setting (Fig. 10); character- istic values of the Vp/Vs ratio and the Moho depth are summarized in Table 2 for each crustal block, together with results of previous regional

studies. The resulting Hk-stacks are illustrated for typical areas in south- ern Africa in Fig. 11 and the entire set of stacks is documented in Fig. S4. We next discuss the crustal blocks from north to south; additional tec- tonic details and the corresponding references are already provided in Section 2.

6.1.1. Central Zimbabwe Craton (Tokwe block), block Z1

This ancient crustal block made of ca. 3.5 Ga gneisses has a relatively thin crust (35–38 km thick) and Vp/Vs ratio of 1.74–1.79. The Tokwe block could represent an "undisturbed" Archean crust, given that the latest known major tectonic event that affected this part of the Zimbabwe Craton was the emplacement of the Great Dyke in the late Archean. This conclusion is supported by geochemical studies of mantle xenoliths which indicate the presence of extremely depleted litho- spheric mantle beneath the southern margin of the Tokwe block (Smith et al., 2009). However, the moderately thin cratonic crust and the extremely sharp Moho transition (Fig. 8) may indicate that a pre- existing lower crust was delaminated in a way similar to that proposed for the Paleozoic Hercynian crust in Europe (cf. Artemieva and Meissner, 2012).

6.1.2. Western Zimbabwe Craton (Tati block), block Z2

In contrast to the Tokwe block, this crustal block has a deep Moho (47–51 km) but a similar Vp/Vs ratio (1.75–1.77). The thick crust at this western margin of the Zimbabwe Craton can be related to deforma- tion and metamorphism of the Archean rocks, similar to Kheis Belt along the western margin of the Kaapvaal Craton (block K1). Although this part of the Zimbabwe Craton has been affected by the Okavango dyke swarm, the Vp/Vs ratio is similar to the Tokwe block, which indicates similar average crustal composition and therefore relatively shallow manifestation of this magmatic event. However, the Moho has a very gradual structure along the whole area affected by the Okavango Dyke Swarm in this block and the Limpopo Belt, which could indicate mag- matic modification of the lower portions of the crust, e.g., by simulta- neous intrusion of very large volumes of magma as an underplated layer around Moho, which by slow cooling due to its large volume

created a gradual transition. Similar observation has been made at a large batholith in the North Sea area (Sandrin and Thybo, 2008a, 2008b).

6.1.3. Limpopo Belt (LB), blocks L1–L2

Our results do not allow distinguishing the central and the marginal zones of the LB by variations in the crustal structure. However, the LB clearly splits into two crustal blocks with similar crustal thickness (42–46 km) but significantly different Vp/Vs ratios. Some crustal thickening, observed in several regional RF studies (Fig. 7), can be the result of the collisional event (ca. 2.7 Ga) by which the LB was formed. The central-western part of the LB has "normal" Vp/Vs of 1.70–1.74. In contrast, the eastern block (labeled L1) has highly heterogeneous composition with extreme values of 1.90–1.93 at several stations. This anomalously high Vp/Vs ratio, also observed at one station at the southern margin of the Zimbabwe Craton, is apparently associated with the "triple junction" of the Okavango and Save-Lebombo Dyke Swarms (Burke and Dewey, 1973) and may result from voluminous magmatic intrusions into the crust. The parts of the Limpopo Belt that were affected by the Okavango Dyke Swarm have a very gradual Moho transition, cf. block Z2, but the highest Vp/Vs ratio is observed in L2, where the Moho is relatively sharp.

6.1.4. Bushveld Intrusion Complex (BIC), blocks B1–B3

BIC is exposed only in the western and eastern parts (blocks B2 and B3, respectively); its existence in the central part (block B1) has been proposed based on gravity modeling (e.g., Webb et al., 2004). Our results indicate that the crustal structure of the three blocks is significantly different (Table 2), both in crustal thickness and in average crustal composition, although the whole complex has gradual, non-sharp Moho transition. The central part (block B1) has a clear minimum in Vp/Vs ratio (1.68–1.70) indicative of an overall felsic composition of the crust. It is flanked by areas (B2 and most of B3) with "normal" Vp/Vs ratio (1.74), whereas the easternmost part of block B3 has very high Vp/Vs = 1.83–1.84. The latter block, affected by the Olifants River Dyke Swarm, is dominated by mafic composition of the crust, suggesting that (in contrast to the Tati block of the Zimbabwe Craton) magmatism has modified much of the 44–49 km thick crustal column. The western BIC lobe (block B2) has a typical continental crustal thickness of 39–42 km, whereas the central BIC (block B1) has the deepest Moho within the Bushveld area, 45 km to 50 km. A similar thick crust is observed in other Archean regions worldwide, such as in the Medicine Hat-Wyoming blocks in the Canadian Shield (Clowes et al., 2002) and in the Anabar Shield in Siberia (Cherepanova et al., 2013). We argue that, given its overall felsic composition, the thick crust in Central Bushveld may mark a paleocollisional zone rather than an intrusion. As an analog one may note that Paleoproterozoic rapakivi granites in the Baltic shield form a semicircle around a deep crustal root in Central Finland, at the boundary between the Archean and the Paleoproterozoic terranes (Artemieva and Thybo, 2013; Artemiev et al., 2006). Similarly, the crustal root in Central Bushveld may have deflected rising magmas sideward, leading to the formation of two lobes of the intrusive complex.

6.1.5. Ancient terranes in NE Kaapvaal, blocks PGM and BGB

The Pietersburg–Giyani–Murchison block (PGM) and the Barberton Greenstone Belt (BGB), which represent the most ancient crust in the southern African region (ca. 3.4–3.7 Ga), have markedly different crustal structure. Both terranes represent remnants of extensive fold and thrust belts with complex, but different polyphase tectonic histories. The PGM block has a relatively thin crust (34–39 km), uniform Vp/Vs of 1.74 and a gradual Moho transition, whereas the BGB block has a deeper Moho (44 km, one station only) and higher Vp/Vs ratio of 1.77, which corresponds to a more mafic composition of the crust. The PGM and BGB blocks are separated by crust, which was significantly modified by the Olifants River Dyke Swarm (the eastern block of BIC, B3). The southern boundary of the PGM block corresponds to the Thabazimbi–

Murchison Lineament, which is not only a surface feature (Thomas et al., 1993) but clearly is a significant crustal-scale tectonic element.

6.1.6. NW Kaapvaal Craton (the Gaborone Granites), block G

This area has a 41–46 km depth to Moho (Moho is sharp) and a high Vp/Vs ratio of 1.77–1.80 with a strong signal from the mid-crustal discontinuity as well as a relatively sharp Moho transition. Thick crust and high Vp/Vs may be related to the Eburnian orogeny (ca. 2.0 Ga) along the western margin of the Kaapvaal Craton (the last major tectono-magmatic event in the area), which led to deformation of the Archean rocks and metamorphism. Crustal thickening during collisional tectonics could have been accompanied by emplacement of mantle-derived magmas into the base of the crust which, in turn, promoted anatexis of depleted protoliths suitable for the generation of A-type granites (Key and Wright, 1982; Moore et al., 1993).

6.1.7. Central Kaapvaal (the Witwatersrand Basin), block W

This block has a crustal thickness of 38–40 km and a Vp/Vs ratio of 1.75–1.78. Some crustal thinning as compared to crustal blocks to the north and a shift towards a more mafic crustal composition can be ancient features (ca. 2 Ga old) produced in response to either the Vredefort impact or to the Ventersdorp-LIP tectono-magmatic event. Particularly, magmatic intrusions associated with the Ventersdorp rifting could be partially responsible for Proterozoic basin subsidence.

6.1.8. The Vredefort crater, block V1

The crater is located in the heart of the Witwatersrand Basin, where the impact event (2.023 Ga) has exposed most of the ca. 3.1 Ga crust, probably down to the crust–mantle transition (Hart et al., 1990a). Given a unique exposure of a complete crustal section, it is often used as a benchmark cross-section of the typical Archean crust, including crustal composition and concentration of heat producing elements (Lana et al., 2003; Rudnick and Fountain, 1995). Our results demonstrate that this crustal cross-section is non-representative of Archean crustal structure. The Vredefort crater has an anomalously shallow Moho at a depth of 34 km and an anomalously high Vp/Vs ratio of
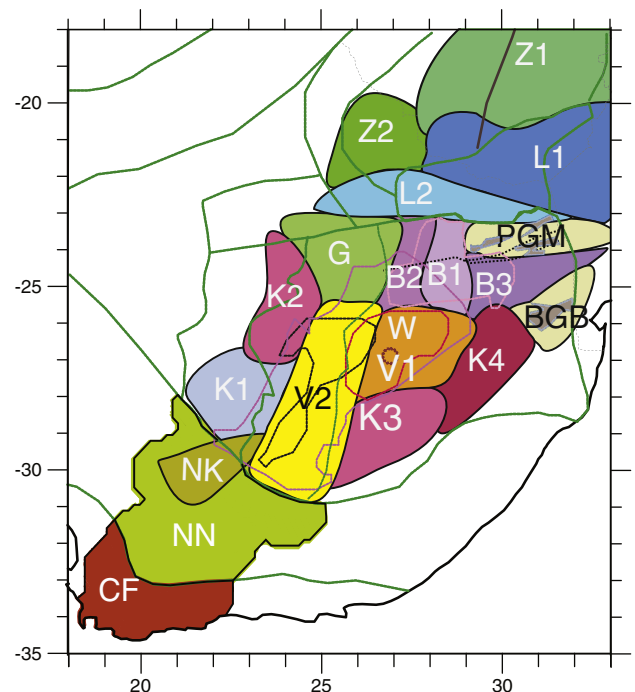

Fig. 10. Crustal blocks identified from the maps of Moho depth and Vp/Vs (see Section 6 and Table 2 for details).

Table 2
Crustal blocks recognized by the Vp/Vs ratio, Moho depth and Moho sharpness.

Block name	Location	Typical Moho depth (km) (present study)	Typical Vp/Vs ratio (present study)	Moho depth (km) from other studies	Vp/Vs (Nair et al., 2006)	Moho sharpness
Z1	Central Zimbabwe Craton (Tokwe block)	35–38	1.74–1.79	37–38 N06 35–38 KG 36–38 K09 37–38 Y08	1.70–1.74	Very sharp
Z2	Western Zimbabwe Craton (Tati block and Okavango dyke swarm)	47–51	1.75–1.77	47–52 N06 49–51 KG 48–51 K09 40–44 Y08	N/A	Gradual
L1	Eastern Limpopo Belt (LP), intersection of dyke swarms	42–46 (one station; 35)	1.79–1.93	39–50 N06 38–51 KG 38–46 K09 38–42 Y08	1.72–1.74	Very gradual
L2	Central Limpopo Belt (LP)	43–45	1.70–1.74	50–53 N06 49–51 KG 47–50 K09 44 N01 + 43–44 Y08	1.74–1.75	Sharp
B1	Bushveld Intrusion Complex (BIC), central part	45–50	1.68–1.7	47–49 N06 44–45 KG 38–46 K09 44–50 N01 42–43 Y08	N/A	Gradual
B2	Bushveld Intrusion Complex, western lobe	39–42	1.74	39–49 N06 43–45 KG 38–41 K09 44–50 N01 42–44 Y08	1.73–1.82	Gradual
B3	Bushveld Intrusion Complex, eastern lobe and Olifants river dyke swarm	44–49	1.83–1.84	43–54 N06 38–45 KG 38–46 K09 42–45 N01 42–43 Y08	N/A	Gradual
PGM	Pietersburg–Giyani–Murchison (PGM)	34–39	1.74	38–44 N06 36–43 KG 36–43 K09 38–43 N01 39–40 Y08	1.73–1.75	Gradual
BGB	Barberton Greenstone Belt (BGB)	44	1.72–175	37–39 N06 38 K09 36–37 Y08	1.77	Relatively sharp
G	North-Western Kaapvaal Craton (Gaborone granites)	41–46	1.77–1.80	41–44 N06 43–45 KG 43–46 K09 40–47 N01 40–43 Y08	1.76–1.81	Relatively sharp
W	Central Kaapvaal (Witwatersrand basin)	38–40	1.75–1.78	38–45 N06 40–45 KG 36–43 K09 42–45 N01 37–41 Y08	1.73–1.75	Relatively sharp
V1	Vredefort crater	34	1.8	38 N06 38 K09 37 Y08	1.73 (assumed value, not calculated)	Sharp
V2	Western Kaapvaal (Ventersdorp rift & LIP)	34–39	1.67–1.73	34–40 N06 38–40 KG 33–40 K09 33–44 N01 36–40 Y08	1.70–1.77	Very sharp
K1	Southern Kheis (one station)	48	1.91	35–40 N06 36–43 K09 35–40 N01 38–41 Y08	1.75–1.76	Gradual
K2	Northern Kheis/Okwa	34–35	1.74	35–43 N06 33–43 K09 34–46 N01 38–40 Y08	1.72–1.77	Relatively Sharp
K3	South–Eastern Kaapvaal Craton	35–36	1.74	36 N06 36 K09 37–40 N01 36–38 Y08	1.76–1.77	Sharp
K4	South-Central Kaapvaal Craton	39–41	1.71–1.74	36–39 N06 36–38 K09 28–42 N01 36–38 Y08	1.72–1.77	Very sharp

Table 2 (*continued*)

Block name	Location	Typical Moho depth (km) (present study)	Typical Vp/Vs ratio (present study)	Moho depth (km) from other studies	Vp/Vs (Nair et al., 2006)	Moho sharpness
NK	Southern border of Kheis Belt with NNMB	40–43	1.66–1.69	37–44 N06 40–41 K09 37–45 N01 38–42 Y08	1.70–1.73	Gradual
NN	Namaqua–Natal Mobile Belt (NNMB)	41–48	1.69–1.78 (one station; 1.95)	41–49 N06 28–46 K09 39–48 Y08	1.70–1.74	Gradual
CF	Cape Fold Belt (CFB)	34–48	1.60–1.90	30–49 N06 26–36 K09 36–42 Y08	N/A	Variable to sharp

KG: Kgaswane et al. (2012) and Gore et al. (2009).
K09: Kgaswane et al. (2009).
N01: Nguuri et al. (2001).
N01+: Nguuri et al. (2001) cover the block partially.
N0*: Nguuri et al. (2001) cover the southern part of the block.
Y08: Yang et al. (2008).
N06: Nair et al. 2006.

1.80. As in other large meteoritic shock-related structures, the crust has been subject to high-pressure metamorphism which led to a significant local increase of the Vp/Vs ratio, not observed at the other adjacent stations (Fig. 9). This anomalous Vp/Vs ratio can also, at least in part, be caused by erosion of the upper crust after the impact and/or by metamorphism associated with impact-caused local heating. This conclusion is supported by the presence of massive to foliated metamorphosed granitoids (ca. 3.0 Gy old) in a 10 km thick middle crustal layer, which overlie a 3.5 Gy old gneiss complex of the lower crust (Hart et al., 1990b; Moser et al., 2001; Stepto, 1990).

6.1.9. Western Kaapvaal (the Ventersdorp rifting and LIP), block V2

This crustal block includes the area affected by two consequent large-scale intracontinental thermal events: (1) rifting at ca. 2.7 Ga and (2) the emplacement of flood basalts (LIP), probably as a result of the second rifting episode at ca. 2.05 Ga. A relatively thin crust (Moho at 34–39 km depth) in the block is typical of Phanerozoic extensional regions. A composite reflection seismic section of the Kaapvaal Craton constrained by eight deep-seismic reflection profiles (de Wit and Tinker, 2004) suggests that regional extensional tectonism affected the entire crust and probably parts of the lithospheric mantle from which at least some of the extensive basaltic–komatiitic volcanics of the Ventersdorp may have been derived (Meyers et al., 1990). However, in contrast to expectations, low Vp/Vs ratio of 1.69–1.73 rules out the presence of voluminous mafic intrusions in the crust. This conclusion is supported by the absence of mafic granulites in the lower crustal xenoliths (Schmitz and Bowring, 2003). Other RF studies reported similar values of Vp/Vs = 1.74 (σ = 0.254) and Vs = 3.71 km/s in the Kimberley block (e.g., Niu and James, 2002) and support the widely accepted view that a mafic lower crustal layer is lacking beneath this part of the Kaapvaal Craton (Durrheim and Green, 1992), except for some intruded ultramafic–mafic bodies (Nair et al., 2006). The latter interpretation, however, does not explain the presence of the intra-crustal discontinuity (Fig. 5). We propose that the relatively thin crust and low Vp/Vs ratio in the region affected by large-scale rifting indicate delamination of the lower crust and mantle lithosphere in Late Archean–Paleoproterozoic time. However, also extension may produce a sharp Moho transition, but the high velocity lower crust would probably be thinned as the rest of the crust and therefore the average crustal velocity should remain higher after extension than after delamination. The Moho transition in block V2 is very sharp, similar to K3 and K4, which support the delamination hypothesis. This hypothesis does not contradict Re–Os isotope data on the ages of the mantle lithosphere in the Jagersfontein and Kimberley kimberlites where Re-depletion model ages older than 2.7 Ga are not documented (Pearson, 1999). Our interpretation fundamentally disagrees with the hypothesis of James et al. (2003) who tagged this area as the "undisturbed" Archean crust.

6.1.10. Southern Kheis Belt, block K1

Although this block has only one seismic station (SA 22), we distinguish it by a deep Moho (48 km), extremely high Vp/Vs = 1.91 and a gradational Moho transition. The station shows a clear signal for crustal layering with a ca. 16 km thick lower crust, in agreement with the earlier observation of the thick, high-Vs lower crust (Yang et al., 2008). We interpret this crustal structure to represent a paleo-suture related to deformation and metamorphism of the Archean rocks along the western margin of the Kaapvaal Craton.

6.1.11. Northern Kheis/Okwa and SE Kaapvaal, blocks K2–K3

These blocks have markedly similar crustal parameters, with a uniformly thin cratonic crust with a thickness of 34–35 km, a uniform normal Vp/Vs ratio of 1.74 and a sharp Moho transition. This similarity may indicate that a pre-existing tectonic block including the two regions became separated at surface by the Ventersdorp LIP province. The crustal thickness is similar to the Ventersdorp LIP but the Vp/Vs ratio, surprisingly, is higher. Crustal thinning in blocks K2–K3 may be associated with delamination processes and extensional tectonics in the Ventersdorp province, which however only weakly affected the overall crustal composition in the adjacent crustal blocks.

6.1.12. Western-Eastern Kaapvaal boundary (between blocks V2 and W/K3)

The boundary is marked by the Colesberg Magnetic Lineament (CML) (Schmitz et al., 2004). It manifests subduction-related and collisional processes (2.7–2.9 Ga) and separates the late and the Mid-Archean blocks of Kaapvaal. Our high-resolution model indicates high Vp/Vs = 1.76 around the CML and the collisional boundary between the Western and Eastern Kaapvaal (Fig. 9a). This feature is not, however, expressed in the Moho depth variations.

6.1.13. South-Central Kaapvaal Craton, block K4

One more crustal block in the Kaapvaal is recognized by a deep Moho (at 39–41 km), although the Vp/Vs ratio (1.71–1.74) and the very sharp Moho transition are similar to blocks K2–K3. This crustal structure is similar to many parts of the East European and the Siberian Cratons (Artemieva and Thybo, 2013; Cherepanova et al., 2013, and references therein) and the Canadian shield (Darbyshire et al., 2007) and thus is a candidate for a typical Archean crust.

6.1.14. Kheis–Namaqua–Natal border, block NK

This block marks the transition between the Kheis Belt and the NNMB and is characterized by an extremely low Vp/Vs ratio of 1.66–
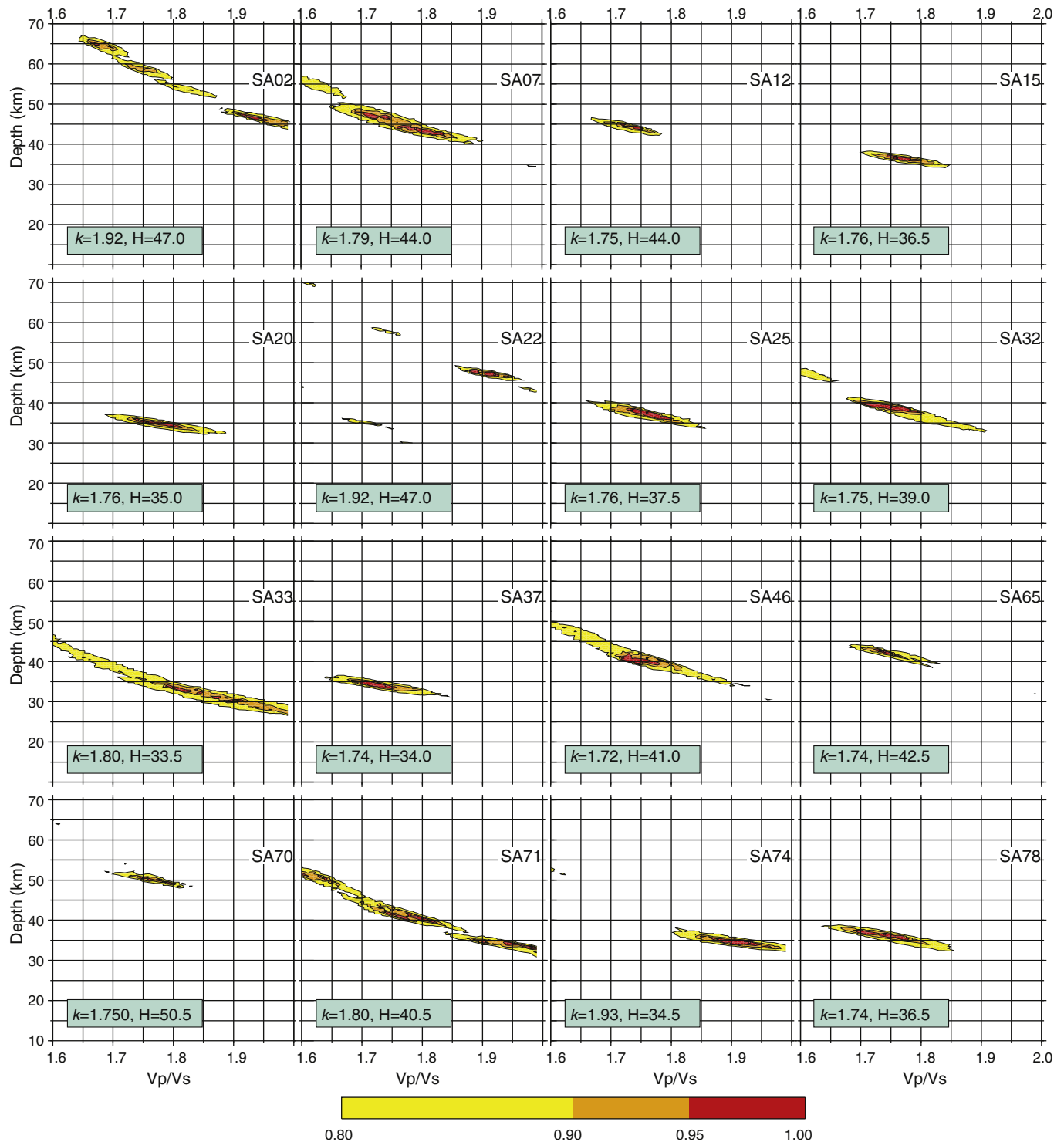
Fig. 11. Average crustal thickness and Vp/Vs ratio estimation using Hk-stacking analysis for selected stations. Contour plots of the Hk-stacking analysis for all stations used in southern Africa are shown in Supplementary Fig. S4.

1.69 and a slightly deeper Moho (40–43 km) than in adjacent crustal blocks. The Vp/Vs ratio is the lowest for the entire southern Africa and suggests that no mafic crust is present.

6.1.15. Namaqua–Natal Mobile Belt (NNMB), block NN

This region has a highly heterogeneous crustal structure. Typically the crust is thick (41–48 km) and Vp/Vs is in the range of 1.69–1.78 with one anomalous station (SA08) with the highest value in the area (Vp/Vs =

1.95 with crustal thickness of 48 km). Thick crust and high Vp/Vs are typical of a collisional belts with a possible mafic intrusive component, e.g., mafic granulites (Dawson and Smith, 1987). This interpretation is also in agreement with the observed gradual Moho transition.

6.1.16. Cape Fold Belt (CFB), block CF

Similar to NNMB, the crust of this fold belt is highly heterogeneous with the Moho depth ranging from 34 to 48 km and Vp/Vs

ratio between 1.60 and 1.90. Strong crustal heterogeneity reflects a mosaic of crustal terranes with different origin and ages (including some Precambrian blocks) which were amalgamated during the assembly of Pangea.

6.2. Comparison to crustal structure in other cratons

Our results indicate large regional variability in the Moho depth beneath the Kalahari Craton, with values ranging from 33 to 35 km to ca. 50 km in the Kaapvaal and Zimbabwe Cratons and up to ca. 55 km in the Limpopo Belt (Table 1). Although the range of these values fully corresponds to the typical range of the Moho depth variations observed globally in other Archean terranes, the variability in the crustal thickness values at craton-scale is extreme in southern Africa. Similar heterogeneity in the crustal structure has been reported for the Indian shield (Julia et al., 2009), which split from southern Africa during the breakup of Pangea. In particular, joint inversion of PRFs with Rayleigh-wave group velocities demonstrate significant variations in the crustal thickness and low crustal S-wave velocities in India, with the Moho depth ranging from 32 to 35 km beneath the Archean East Dharwar and Bundelkhand Cratons (with lower crustal velocities around 3.8–3.9 km/s), over 45–50 km in the Archean West Dharwar Craton and Southern Granulite Terrane, and to 50–65 km in the Proterozoic crust of the Bhandara Craton and the Aravalli–Delhi Belt, where lower crustal velocities are around 4.2–4.3 km/s. This pattern is similar to southern Africa, where crustal blocks with an (apparently) extended or delaminated lower crustal layer have thin crust as compared to magmatically and tectonically reworked Archean–Proterozoic crust.

Significant variations in the Moho depth are also reported for the Canadian shield (e.g., Clowes et al., 2002; Darbyshire et al., 2007; Keller, 2013), the East European Craton (including its exposure in the Baltic shield) (Artemieva and Thybo, 2013), the Siberian Craton (Cherepanova et al., 2013), and Precambrian Australia (Salmon et al., 2013). Crustal thickness varies in a smaller range of 36–42 km in the smaller-size Tanzanian Craton (Last et al., 1997). We thus conclude that significant short-wavelength variability in the crustal thickness is an inherent feature of the cratonic crust which reflects the complex history of its formation, amalgamation, and tectono-magmatic reworking.

Our results demonstrate that the composition of the cratonic crust is also significantly heterogeneous. This finding is in contrast to recent results from the Indian shield where rather uniform Poisson's ratios close to 0.25 were determined (Kumar et al., 2001; Saul et al., 2000). Similarly, low values were estimated for the Archean Tanzanian Craton (σ = 0.24–0.26) and the Proterozoic Arabian shield (Kumar et al., 2002; Last et al., 1997), suggesting that Poisson's ratios close to 0.25 may be more characteristic of the Precambrian crust than the higher value of 0.29 (Zandt and Ammon, 1995). Although low Poisson's ratios are also consistent with the estimated average continental crust composition with 59% silica content (Rudnick and Fountain, 1995), our results for southern Africa demonstrate that Archean terranes with low Vp/Vs may have lost a significant portion of the lower crust. At the same time, the existence of Archean terranes with very high Vp/Vs ratio questions the possibility of tagging any Archean block as "typical" or "undisturbed" cratonic crust.

7. Conclusions

We present new results on the crustal structure, Moho depth and crustal composition in the southern African Cratons. Based on the results from calculating 6300 RFs for the entire SASE dataset at 85 stations, we develop a new detailed regional model of crustal thickness and Vp/Vs ratio variations. The current model has a higher resolution than previous studies. This advantage arise from analyzing the crustal parameters using full Hk-stacking interpretations along with multi-frequency bands of the data recorded by all 85 broadband seismic stations.

Increased resolution allows imaging of small-scale features that the previous studies were unable to image.

The southern African crust is characterized by considerable heterogeneity with short wavelength variations in crustal thickness, composition and Moho structure, and it shows the presence of a mid-crustal discontinuity within some cratonic blocks.

Data on the depth to Moho and Vp/Vs ratio allows us to distinguish ca. 20 crustal blocks divided by boundaries, which do not everywhere follow terrane boundaries recognized from surface tectonics. The following major crustal features are recognized from north to south:

- Zimbabwe Craton: The Tokwe block with H = 35–38 km and k = 1.74–1.79 may potentially represent "undisturbed" Archean crust, although a pre-existing lower crust may have been delaminated, whereas crustal thickening in the Tati block (H = 47–51 km) can be related to deformation of the Archean crust along the cratonic margin.
- Limpopo Belt: Two distinct crustal blocks with a similar crustal thickness (42–46 km) but significantly different Vp/Vs ratios are recognized. Extreme values of 1.90–1.93 in the eastern part indicate voluminous magmatic additions to the crust associated with the "triple junction" of regional dyke swarms.
- Bushveld Intrusion Complex (BIC): High Vp/Vs of ca. 1.84 is typical of the easternmost lobe of the complex, where the entire crustal column further has been modified by the Olifants River Dyke Swarm. We do not find evidence for magmatic intrusions in the central (inferred) part of BIC, where the crust is thick (45–50 km) and Vp/Vs is low (1.68–1.70). Thick crust with an overall felsic composition, typical of a paleocollisional zone, suggests that a crustal root may have deflected raising magmas sideward, leading to the formation of two lobes of BIC.
- Kaapvaal Craton: Most of the central craton has thin (35–40 km) crust and Vp/Vs around 1.74, except for the Ventersdorp terrane where Vp/Vs = 1.67–1.73. The thin crust and low Vp/Vs ratio indicate possible delamination of the lower crust and mantle lithosphere caused by series of large-scale Precambrian rifting events.
- Vredefort impact crater: The shallow Moho (34 km) and anomalously high Vp/Vs (1.80) may be attributed to shock metamorphism, and the exposed crustal cross-section therefore is non-representative of the cratonic crust.
- Witwatersrand Basin and Colesberg Magnetic Lineament have typically high k = 1.76, whereas the SW Kaapvaal/Kheis/Namaqua transition has anomalously low Vp/Vs = 1.66–1.67.
- Namaqua–Natal and Cape Fold Belts both have a highly heterogeneous crust, regarding both crustal thickness and Vp/Vs ratio.

We interpret the sharp Moho in thin crust with small Vp/Vs as an indication that some portions of the Archean Cratons in southern Africa have lost their lower crust during their evolution, possibly by delamination processes that would remove the most mafic parts of the crust and leave a felsic crust with the characteristic low Vp/Vs.

The results of the present study demonstrate that the cratonic crust represents a mosaic of blocks with variable thickness and composition that were formed and reshaped by an interplay of different tectonothermal processes that were active during and after craton formation. Our observation of extreme short-wavelength structural and compositional heterogeneity of the cratonic crust in southern Africa, as well as in other cratonic regions worldwide, shows that "typical" cratonic crust cannot be defined.

Supplementary data to this article can be found online at http://dx.doi.org/10.1016/j.tecto.2013.09.001.

References

Aki, K., Richards, P.G., 2002. Quantitative Seismology, 2nd edn. University Science Books, Sausalito, CA.

Altermann, W., Halbich, I.W., 1991. Structural history of the southwestern corner of the Kaapvaal Craton and the adjacent Namaqua realm: new observations and a reappraisal. Precambrian Res. 52, 133–166.

Amelin, Y., Lee, D.C., Halliday, A.N., Pidgeon, R.T., 1999. Nature of the Earth's earliest crust from Hafnium isotopes in single detrital zircons. Nature 399, 252–255.

Ammon, C.J., 1991. The isolation of receiver effects from teleseismic P waveforms. Bull. Seismol. Soc. Am. 81, 2504–2510.

Arculus, R.J., 1999. Origins of the continental crust. J. Proc. R. Soc. NSW 132, 83–110.

Artemieva, I.M., Thybo, H., 2008. Deep Norden: highlights of the lithospheric structure of Northern Europe, Iceland, and Greenland. Episodes 31, 98–106.

Artemieva, I.M., Meissner, R., 2012. Crustal thickness controlled by plate tectonics: A review of crust–mantle interaction processes illustrated by European examples. Tectonophysics 530–531, 18–49.

Artemieva, I.M., Thybo, H., 2013. EUNAseis: a seismic model for Moho and crustal structure in Europe, Greenland, and the North Atlantic region. Tectonophysics. http://dx.doi.org/10.1016/j.tecto.2013.1008.1004.

Artemieva, I.M., Thybo, H., Kaban, M.K., 2006. Deep Europe today: geophysical synthesis of the upper mantle structure and lithospheric processes over 3.5 Ga. In: Gee, D.a., R., S. (Eds.), European Lithosphere Dynamics. Geological Society London Spec. Publ., London, pp. 11–41.

Barton, J.M., Klemd, R., Zeh, A., 2006. The Limpopo Belt: a result of Archean to Proterozoic. Turkic-type orogenesis? . GSA Special Papers 2006, vol. 405, pp. 315–332.

Burke, K., Dewey, J.F., 1973. Hot spots and continental breakup: implications for collisional orogeny. Geology 2, 57–60.

Burke, K., Kidd, W.S.F., Kusky, T.M., 1985. Is the Ventersdorp rift system of southern Africa related to a continental collision between the Kaapvaal and Zimbabwe Cratons at 2.64 Ga ago? Tectonophysics 115, 1–24.

Cahen, L., Snelling, N.J., Delhal, J., Vail, J.R., 1984. The Geochronology and Evolution of Africa. Clarendon Press, Oxford.

Carlson, R.W., Grove, T.L., de Wit, M.J., Gurney, J.J., 1996. Anatomy of an Archean Craton: a program for interdisciplinary studies of the Kaapvaal Craton, southern Africa. EOS Trans. Am. Geophys. Union 77, 273–277.

Cawthorn, R.G., Walraven, F., 1998. Emplacement and crystallization time for the Bushveld Complex. J. Petrol. 39, 1669–1687.

Cherepanova, Y., Artemieva, I., Thybo, H., Chemia, Z., 2013. Crustal structure of the Siberian Craton and the West Siberian basin: an appraisal of existing seismic data. Tectonophysics. http://dx.doi.org/10.1016/j.tecto.2013.1005.1004.

Chevrot, S., van der Hilst, R.D., 2000. The Poisson ratio of the Australian crust: geological and geophysical implications. Earth Planet. Sci. Lett. 183, 121–132.

Chevrot, S., Zhao, L., 2007. Multiscale finite-frequency Rayleigh wave tomography of the Kaapvaal Craton. Geophys. J. Int. 169 (1), 201–215.

Clarke, T.J., Silver, P.G., 1993. Estimation of crustal Poisson's ratio from broad band teleseismic data. Geophys. Res. Lett. 20 (3), 241–244.

Clayton, R.W., Wiggins, R.A., 1976. Source shape estimation and deconvolution of teleseismic body waves. Geophys. J. R. Astron. Soc. 47, 151–177.

Clifford, T.N., 1970. The structural framework of Africa. In: Clifford, T.N., Gass, I.G. (Eds.), African Magmatism and Tectonics. Oliver and Boyd, Edinburgh, pp. 1–26.

Clowes, R.M., Burianyk, M.J.A., Gorman, A.R., Kanasewich, E.R., 2002. Crustal velocity structure from SAREX, the Southern Alberta refraction experiment. Can. J. Earth Sci. 39, 351–373.

Condie, K.C., 1997. Plate Tectonics and Crustal Evolution. Butterworth Heinemann, Oxford (282 p.).

Cooper, M.R., 1990. Tectonic cycles in southern Africa. Earth Sci. Rev. 28, 321–364.

Dahlen, F.A., Tromp, J., 1998. Theoretical Global Seismology. Princeton University Press, Princeton.

Dahl-Jensen, T., et al., 2003. Depth to Moho in Greenland: Receiver-function analysis suggests two Proterozoic blocks in Greenland. Earth Planet. Sci. Lett. 205, 379–393.

Darbyshire, F.A., Eaton, D.W., Frederiksen, A.W., Ertolahti, L., 2007. New insights into the lithosphere beneath the Superior Province from Rayleigh wave dispersion and receiver function analysis. Geophys. J. Int. 169, 1043–1068.

Dawson, J.B., Smith, J.V., 1987. Reduced sapphirine granulite xenoliths from the Lace kimberlite, South Africa: Implications for the deep structure of the Kaapvaal Craton. Contrib. Mineral. Petrol. 95, 376–383.

De Beer, J.H., 1983. Geophysical studies In the southern Cape Province and models of the lithosphere In the Cape Fold Belt. Spec. Publ. Geol. Soc. S. Afr., 12 57–64.

de Wit, M.J., Tinker, J., 2004. Crustal structures across the central Kaapvaal Craton from deep-seismic reflection data. S. Afr. J. Geol. 107, 185–206.

de Wit, M.J., Roering, C., Hart, R.J., Armstrong, R.A., de Ronde, C.E.J., Green, R.W.E., Tredoux, M., Peberdy, E., Hart, R.A., 1992. Formation of an Archaean continent. Nature 357, 553–562.

Dueker, K.G., Sheehan, A.F., 1998. Mantle discontinuity structure beneath the Colorado Rocky Mountains and High Plains. J. Geophys. Res. 103, 7153–7169.

Durrheim, R.J., Green, R.W., 1992. A seismic refraction investigation of the Archean Kaapvaal Craton, South Africa, using mine tremors as the energy source. Geophys. J. Int. 108, 812–832.

Durrheim, R.J., Mooney, W.D., 1991. Archean and Proterozoic crustal evolution; evidence from crustal seismology. Geology (Boulder) 19 (6), 606–609.

Durrheim, R.J., Barker, W.H., Green, R.W.E., 1992. Seismic studies in the Limpopo Belt. Precambrian Res. 55, 187–200.

Fyfe, W.S., 1978. The evolution of the Earth's crust: modern plate tectonics to ancient hot spot tectonics? Chem. Geol. 23, 89–114.

Good, N., de Wit, M.J., 1997. The Thabazimbi–Murchison lineament of the Kaapvaal Craton, South Africa: 2700 Ma of episodic deformation. J. Geol. Soc. Lond. 154, 93–97.

Gore, J., James, D.E., Zengeni, T.G., et al., 2009. Crustal structure of the Zimbabwe Craton and the Limpopo Belt of southern Africa: new constraints from seismic data and implications for its evolution. S. Afr. J. Geol. 112, 213–228.

Green, R.W.E., Durrheim, R.J., 1990. A seismic refraction investigation of the Namaqualand Metamorphic Complex, South Africa. J. Geophys. Res. 95 (B12), 19927–19932.

Griffin, W.L., O'Reilly, R.S.Y., 1987. Is the continental Moho the crust–mantle boundary? Geology (Boulder) 15, 241–244.

Gupta, S., Rai, S.S., Prakasam, K.S., et al., 2003. The nature of the crust in southern India: implications for Precambrian crustal evolution. Geophys. Res. Lett. 30 (8), 1419.

Gurrola, H., Minster, J.B., Owens, T., 1994. The use of velocity spectrum for stacking receiver functions and imaging upper mantle discontinuities. Geophys. J. Int. 117, 427–440.

Gurrola, H., Baker, G.E., Minster, J.B., 1995. Simultaneous time domain deconvolution with application to the computation of receiver functions. Geophys. J. Int. 120, 537–543.

Hamilton, P.J., Eversen, N.M., O'Nions, R.K., Smith, H.S., Erlank, A.J., 1979. Sm–Nd dating of Onwerwacht Group volcanics, southern Africa. Nature (London) 279, 298–300.

Hart, R.J., Andreoli, M.A.G., Tredoux, M., de Wit, M.J., 1990a. Chem. Geol. 82, 21.

Hart, R.J., Andreoli, M.A.G., Tredoux, M., de Wit, M.J., 1990b. Geochemistry across an exposed section of Archean crust at Vredefort, South Africa: with implications for mid-crustal discontinuities. Chem. Geol. 82, 21–50.

Hawkesworth, C.J., Kemp, A.I.S., 2006. Evolution of the continental crust. Nature 443, 811–817.

Hawkesworth, C., Cawood, P., Dhuime, B., 2013. Continental growth and the crustal record. Tectonophysics. http://dx.doi.org/10.1016/j.tecto.2013.1008.1013.

Holbrook, W.S., Reiter, E.C., Purdy, G.M., Toksoz, M.N., 1992. Image of the Moho across the continent–ocean transition, United States east-coast. Geology 20, 203–206.

James, D.E., Carlson, R.W., Boyd, F.B., Janney, P.E., 2001a. Petrologic constraints on seismic velocity variations in the upper mantle beneath southern Africa. EOS Trans. Am. Geophys. Union 82 (20 (Abstract Suppl.)), S247.

James, D.E., Fouch, M.J., VanDecar, J.C., van der Lee, S., the Kaapvaal Seismic Group, 2001b. Tectonospheric structure beneath southern Africa. Geophys. Res. Lett. 28, 2485–2488.

James, D., Niu, F., Rokosky, J., 2003. Crustal structure of the Kaapvaal Craton and its significance for early crustal evolution. Lithos 71, 413–429.

Jelsma, H.A., Dirks, P.H.G.M., 2002. NeoArchean tectonic evolution of the Zimbabwe Craton. In: Fowler, C.M.R., Ebinger, C.J., Hawkesworth, C.J. (Eds.), The Early Earth: Physical, Chemical, and Biological Development. Geol. Soc. Spec. Publ., 199, pp. 183–211.

Jensen, S.L., Thybo, H., 2002. Moho topography and lower crustal wide-angle reflectivity around the TESZ in southern Scandinavia and northeastern Europe. Tectonophysics 360, 187–213.

Jourdan, F., Feraud, G., Bertrand, H., et al., 2006. Basement control on dyke distribution in Large Igneous Provinces: case study of the Karoo triple junction. Earth Planet. Sci. Lett. 241, 307–322.

Julia, J., Jagadeesh, S., Rai, S.S., et al., 2009. Deep crustal structure of the Indian shield from joint inversion of P wave receiver functions and Rayleigh wave group velocities: implications for Precambrian crustal evolution. J. Geophys. Res. 114 (Article Number: B10313).

Keller, G.R., 2013. The Moho of North America: a brief review focused on recent studies. Tectonophysics. http://dx.doi.org/10.1016/j.tecto.2013.1007.1031.

Kennett, B.L.N., Salmon, M., Saygin, E., AusMoho Working Group, 2011. AusMoho: the variation in Moho depth in Australia. Geophys. J. Int. 187, 946–958.

Key, R.M., Wright, E.P., 1982. The genesis of the Gaborone rapakivi granite complex in southern Africa. J. Geol. Soc. Lond. 139, 109–126.

Kgaswane, E.M., Nyblade, A.A., Julia, J., et al., 2009. Shear wave velocity structure of the lower crust in southern Africa: evidence for compositional heterogeneity within Archaean and Proterozoic terrains. J. Geophys. Res. 114 (Article Number: B12304).

Kgaswane, E.M., Nyblade, A.A., Durrheim, R.J., et al., 2012. Shear wave velocity structure of the Bushveld Complex, South Africa. Tectonophysics 554, 83–104.

Kröner, A., 1976. Proterozoic crustal evolution in parts of southern Africa and evidence for extensive sialic crust since the end of the Archaean. Phil. Trans. R. Soc. Lond. A 280, 541–554.

Kumar, M.R., Saul, J., Sarkar, D., Kind, R., Shukla, A.K., 2001. Crustal structure of the Indian shield: New constraints from teleseismic receiver functions. Geophys. Res. Lett. 28, 1339–1342.

Kumar, M.R., Ramesh, D.S., Saul, J., Sarkar, D., Kind, R., 2002. Crustal and upper mantle stratigraphy of the Arabian shield. Geophys. Res. Lett. 29, 1242–1245.

Kumar, P., et al., 2005. The lithosphere–asthenosphere boundary in the North-Atlantic region. Earth Planet. Sci. Lett. 236, 249–257.

Kumar, P., Kind, R., Priestley, K., Dahl-Jensen, T., 2007. Crustal structure of Iceland and Greenland from receiver function studies. J. Geophys. Res. 112 B03301.

Kwadiba, M.T.O.G., Wright, C., Kgaswane, E.M., Simon, R.E., Nguuri, T.K., 2003. Pn arrivals and lateral variations of Moho geometry beneath the Kaapvaal Craton. Lithos 71, 393–411.

Lana, C., Gibson, R.L., Kisters, A.F.M., Reimold, W.U., 2003. Archean crustal structure of the Kaapvaal Craton, South Africa — evidence from the Vredefort dome. Earth Planet. Sci. Lett. 206, 133–144.

Langston, C.A., 1979. Structure under Mount Rainier, Washington, inferred from teleseismic body waves. J. Geophys. Res. 84, 4749–4762.

Last, R.L., Nyblade, A.A., Langston, C.A., 1997. Crustal structure of the East African Plateau from receiver functions and Rayleigh wave phase velocities. J. Geophys. Res. 102, 24469–24483.

Li, X., Yuan, X., Kind, R., 2007. The lithosphere–asthenosphere boundary beneath the western United States. Geophys. J. Int. 170, 700–710.

Ligorría, J.P., Ammon, C.J., 1999. Iterative deconvolution and receiver function estimation. Bull. Seismol. Soc. Am. 89, 1395–1400.

McCourt, S., Vearncombe, J.R., 1992. Shear zones of the Limpopo Belt and adjacent gran-itoid–greenstone terrains: implications for late Archean collision tectonics in south-ern Africa. Precambrian Res. 55, 553–570.

Mengel, K., Kern, H., 1992. Evolution of the petrological and seismic Moho; implications for the continental crust–mantle boundary. Terra Nova 4, 109–116.

Meyers, R.E., McCarthy, T.S., Bunyard, M., Cawthorn, R.G., Falatsa, T.M., Hewitt, T., Linton, P., Myers, J.M., Palmer, K.J., Spencer, R., 1990. Geochemical stratigraphy of the Klipriviersberg Group volcanic rocks. S. Afr. J. Geol. 93, 224–238.

Moore, M.D., Davis, D.W., Robb, L.J., Jackson, M.C., Grobler, D.F., 1993. Archean rapakivi granite–anorthosite–rhyolite complex in the Witwatersrand basin hinterland, south-ern Africa. Geology 21, 1031–1034.

Moser, D.E., Flowers, R.M., Hart, R.J., 2001. Birth of the Kaapvaal tectosphere 3.08 billion years ago. Science 291, 465–468.

Nair, S.K., Gao, S.S., Liu, K.H., Silver, P.G., 2006. Southern African crustal evolution and com-position: constraints from receiver function studies. J. Geophys. Res. 111, B02304.

Nguuri, T., et al., 2001. Crustal structure beneath southern Africa and its implications for the formation and evolution of the Kaapvaal and Zimbabwe Cratons. Geophys. Res. Lett. 28 (13), 2501–2504.

Niu, F., James, D.E., 2002. Fine structure of the lowermost crust beneath the Kaapvaal Craton and its implications for crustal formation and evolution. Earth Planet. Sci. Lett. 200, 121–130.

Niu, F., Kawakatsu, H., 1998. Determination of the absolute depths of the mantle transi-tion zone discontinuities beneath China: effect of stagnant slabs on mantle transition zone discontinuities. Earth, Planets and Space, 50 965–975.

Oldenburg, D.W., 1981. A comprehensive solution to the linear deconvolution problem. Geophys. J. R. Astron. Soc. 65, 331–357.

Oreshin, S., Vinnik, L, Makeyeva, L., Kosarev, G., Kind, R., Wenzel, F., 2002. Combined analy-sis of SKS splitting and regional traveltimes in Siberia. Geophys. J. Int. 151 (2), 393–402.

Owens, T.J., Zandt, G., Taylor, S.R., 1984. Seismic evidence for an ancient rift beneath the Cumberland plateau, Tennessee: A detailed analysis of broadband teleseismic p waveforms. J. Geophys. Res. 89, 7783–7795.

Park, J., Levin, V., 2000. Receiver functions from multiple-taper spectral correlation esti-mates. Bull. Seismol. Soc. Am. 90, 1507–1520.

Pearson, D.G., 1999. The age of continental roots. Lithos 48, 171–194.

Peltonen, et al., 2006. Multi-stage origin of the lower crust of the Karelian Craton from 3.5 to 1.7 Ga based on isotopic ages of kimberlite-derived mafic granulite xenoliths. Pre-cambrian Res. 147 (1–2), 107–123.

Poppeliers, C., Pavlis, G.L., 2003. Three-dimensional plane wave migration of teleseismic P-to-S converted phases: part 1, theory. J. Geophys. Res. 108, 2112.

Ritzwoller, M.H., Levshin, A.L., 1998. Eurasian surface wave tomography: group velocities. J. Geophys. Res. 103, 4839–4878.

Robinson, E.A., 1954. Predictive Decomposition of Seismic Traces with Applications to Seismic Exploration. (Ph.D. Thesis) M.I.T., Cambridge, MA (Reprinted in Geophysics 32, 1967, 418 – 484).

Rollinson, H.R., 1993. A terrane interpretation of the Archean Limpopo Belt. Geol. Mag. 130, 755–765.

Rudnick, R.L., Fountain, D.M., 1995. Nature and composition of the continental crust; a lower crustal perspective. Rev. Geophys. 33, 267–309.

Rudnick, R.L., Gao, S., 2003. In: Rudnick, R.L. (Ed.), The Crust. Treatise in Geochemistry, vol. 3. Elsevier, Amsterdam, pp. 1–64.

Salmon, M., Kennett, B.L.N., Stern, T., Aitken, A.R.A., 2013. The Moho in Australia and New Zealand. Tectonophysics. http://dx.doi.org/10.1016/j.tecto.2012.1007.1009.

Sandrin, A., Thybo, H., 2008a. Deep seismic investigation of crustal extensional structures in the Danish Basin along the ESTRID-2 profile. Geophys. J. Int. 173, 623–641.

Sandrin, A., Thybo, H., 2008b. Seismic constraints on a large mafic intrusion with implica-tions for the subsidence history of the Danish Basin. J. Geophys. Res. 113, B09402. http://dx.doi.org/10.1029/2007JB005067.

Saul, J., Kumar, M.R., Sarkar, D., 2000. Lithospheric and upper mantle structure of the Indian Shield, from teleseismic receiver functions. Geophys. Res. Lett. 27, 2357–2360.

Schmitz, M.D., Bowring, S.A., 2003. Ultrahigh-temperature metamorphism in the lower crust during Neoarchean Ventersdorp rifting and magmatism, Kaapvaal Craton, southern Africa. Geol. Soc. Am. Bull. 115, 533–548.

Schmitz, M.D., Bowring, S.A., de Wit, M.J., Gartz, V., 2004. Subduction and terrane collision stabilized the western Kaapvaal craton tectosphere 2.9 billion years ago. Earth Planet. Sci. Lett. 222, 363–376.

Sheehan, A.F., Shearer, P.M., Gilbert, H.J., Dueker, K.G., 2000. Seismic migration pro-cessing of P-SV converted phases for mantle discontinuity structure beneath the Snake River Plain, western United States. J. Geophys. Res. 105, 19,055–19,065.

Sheriff, R.E., Geldart, L.P., 1993. Exploration Seismology, 2nd ed. Cambridge Univ, Press, New York.

Shibutani, T., Sambridge, M., Kennett, B., 1996. Genetic algorithm inversion for receiver functions with application to crust and uppermost mantle structure beneath Eastern Australia. Geophys. Res. Lett. 23, 1829–1832.

Smith, C.B., Pearson, D.G., Bulanova, G.P., et al., 2009. Extremely depleted litho-spheric mantle and diamonds beneath the southern Zimbabwe Craton. Lithos 112S, 1120–1132.

Stepto, D., 1990. The geology and gravity field in the central core of the Vredefort struc-ture. Tectonophysics 171, 75–103.

Thomas, R.J., Von Veh, M.W., McCourt, S., 1993. The tectonic evolution of southern Africa: an overview. J. Afr. Earth Sci. 16, 5–24.

Thybo, H., Artemieva, I.M., 2013. Moho and magmatic underplating in continental litho-sphere. http://dx.doi.org/10.1016/j.tecto.2013.1005.1032.

Thybo, H., Perchuc, E., Gregersen, S., 1998. Interpretation in statu nascendi of seismic wide-angle reflections based on EUGENO-S data. Tectonophysics 289, 281–294.

Vinnik, L.P., 1977. Detection of waves converted from P to SV in the mantle. Phys. Earth Planet. Inter. 15, 39–45.

Vinnik, L.P., Farra, V., Kind, R., 2004a. Deep structure of the Afro-Arabian hotspot by S re-ceiver functions. Geophys. Res. Lett. 31, L11608.

Vinnik, L., Reigber, C., Aleshin, I., Kosarev, G., Kaban, M.K., Oreshin, S., Roecker, S., 2004b. Receiver function tomography of the Central Tien Shan. Earth Planet. Sci. Lett. 225 (1–2), 131–146.

Vinnik, L., Kiselev, S., Weber, M., Oreshin, S., Makeyeva, L., 2012. Frozen and active seismic anisotropy beneath southern Africa. Geophys. Res. Lett. 39, L08301.

Von Gruenewaldt, G., Sharpe, M.R., Hatton, C.J., 1985. The Bushveld Complex: introduc-tion and review. Econ. Geol. 80, 803–812.

Webb, S.J., Cawthorn, R.G., Nguuri, T.K., James, D.E., 2004. Gravity modeling of Bushveld Complex connectivity supported by Southern African seismic experiment results. S. Afr. J. Geol. 107, 207–218.

Wever, Th., 1992. Comment on "Archean and Proterozoic crustal evolution: evidence from crustal seismology" by R. Durrheim and W. Mooney. Geology 20, 664–665.

Wright, C., Kwadiba, M.T.O., Simon, R.E., et al., 2004. Variations in the thickness of the crust of the Kaapvaal Craton, and mantle structure below southern Africa. Earth, Planets and Space, 56 125–137.

Yang, Y., Li, A., Ritzwoller, M.H., 2008. Crustal and uppermost mantle structure in south-ern Africa revealed from ambient noise and teleseismic tomography. Geophys. J. Int. 174, 235–248.

Yilmaz, O., 1987. Seismic Data Processing. Society of Exploration Geophysicists, Tulsa, Oklahoma.

Youssof, M., et al., 2013. Strong crustal seismic anisotropy in southern African cratons - a terrane discriminator (in preparation).

Yuan, X., Ni, J., Kind, R., Mechie, J., Sandvol, E., 1997. Lithospheric and upper mantle struc-ture of southern Tibet from a seismological passive source experiment. J. Geophys. Res. 102, 27491–27500.

Zandt, G., Ammon, C.J., 1995. Continental crust composition constrained by measure-ments of crustal Poisson's ratio. Nature 374, 152–154.

Zhu, L., Kanamori, H., 2000. Moho depth variation in southern California from teleseismic receiver functions. J. Geophys. Res. 105, 2969–2980.